Vol. 92 No. 6 pp. 2136–2156 ACTA GEOLOGICA SINICA (English Edition) Dec. 2018

Geochemistry, Geochronology, and Hf isotopic Composition of the Late Paleoproterozoic Lujiapuzi Formation, NE Yan-Liao Rift, Northern Liaoning

LIU Jin[1, 2], ZHANG Jian[1, 2, *], LIU Zhenghong[3], YIN Changqing[1, 2], ZHAO Chen[1, 2], PENG Youbo[4], DOU Shiyong[4] and YANG Zhongjie[4]

1 *School of Earth Sciences and Engineering, Sun Yat-sen University, Guangzhou 510275, Guangdong, China*
2 *Guangdong Provincal Key Lab of Geodynamics and Geohazards, School of Earth Sciences and Engineering, Sun Yat-sen University, Guangzhou 510372, Guangdong, China*
3 *College of Earth Sciences, Jilin University, Changchun 130061, Jilin, China*
4 *Liaoning Survey Academy of Geology and Mineral Resources, Shenyang 110031, Liaoning, China*

Abstract: The metasedimentary Lujiapuzi Formation crops out along the northeastern margin of the North China Craton, close to the Yan-Liao Rift. The age and tectonic setting of the formation, and its relationship with the Yan-Liao Rift are currently unclear. Here we present detrital zircon U-Pb ages, and Hf isotopic and geochemical data for the Lujiapuzi Formation to constrain the timing of deposition, the provenance of the formation, and the regional stratigraphy relationship. Zircon U-Pb dating constrains the timing of deposition of the Lujiapuzi Formation to younger than 1780 Ma, and indicates that most grains were sourced from the Longgang Block and the Paleoproterozoic Liao-Ji Belt. Detailed field investigations and a correlation of the regional stratigraphy reveal that much of the Lujiapuzi Formation is equivalent to the Tuanshanzi Formation in the Yan-Liao Rift; the lower section may represent the earliest sediments deposited within the Fanhe Basin. Based on these results and the findings of previous studies, we suggest that the base of the Changcheng System has an age of 1.80 Ga. Zircon Hf isotopic data indicate that the main period of crustal growth along the northeastern margin of the North China Craton occurred at 3.2–2.5 Ga, with a peak at 2.9–2.7 Ga.

Key words: detrital zircon, crustal growth, Changcheng System, Yan-Liao rift, North China Craton

1 Introduction

The North China Craton (NCC), one of the oldest cratons in the world (Liu et al., 1992, 2008; Liu Dunyi et al., 1994), comprises Archean and Paleoproterozoic metamorphic basement overlain by Mesoproterozoic metasedimentary cover sequences (Lu et al., 2008). Zhao et al. (2005, 2012) divided the NCC into the Western and Eastern blocks, which collided along the Trans-North China Orogen (TNCO) at ca. 1.85 Ga (Fig. 1a; Zhao et al., 2001, 2005, 2010, 2012; Wilde et al., 2002, 2005; Wilde and Zhao, 2005; Santosh et al., 2006, 2007; Santosh, 2010; Zhai and Santosh, 2011). Following amalgamation, the NCC underwent several extensional and rifting events in the late Paleoproterozoic to early Neoproterozoic, forming the Xiong'er, Yan-Liao, and Zha'er tai–Bayan Obo rift zones (Fig. 1a; Zhai et al., 2000, 2015; Zhai Mingguo, 2004; Lu et al., 2008; Peng et al., 2011; Zhai and Santosh, 2011).

The Yan-Liao Rift in the interior of the NCC was the site of a prolonged period of sedimentation and minor volcanism from 1.8 to 1.4 Ga, during which time the late Paleoproterozoic Changcheng Group and the Mesoproterozoic Jixian Group were deposited (Lu et al., 2008; Zhai et al., 2015). Recently, bentonites have been described from the Changcheng and Jixian groups (Gao Linzhi et al., 2007, 2008; Su et al., 2008; Li Huaikun et al., 2009, 2014; Su Wenbo et al., 2010; Tian Hui et al., 2015). Based on these observations and the ages of volcanic rocks in the Tuanshanzi and Dahongyu formations (Li Huaikun et al., 1995; Lu et al., 2002, 2008; Lu Songnian et al., 2003; Hu Junliang et al., 2007; Wang et al., 2015; Zhang Jian et al., 2015), the late

* Corresponding author. E-mail: zhangjian@mail.sysu.edu.cn

© 2018 Geological Society of China

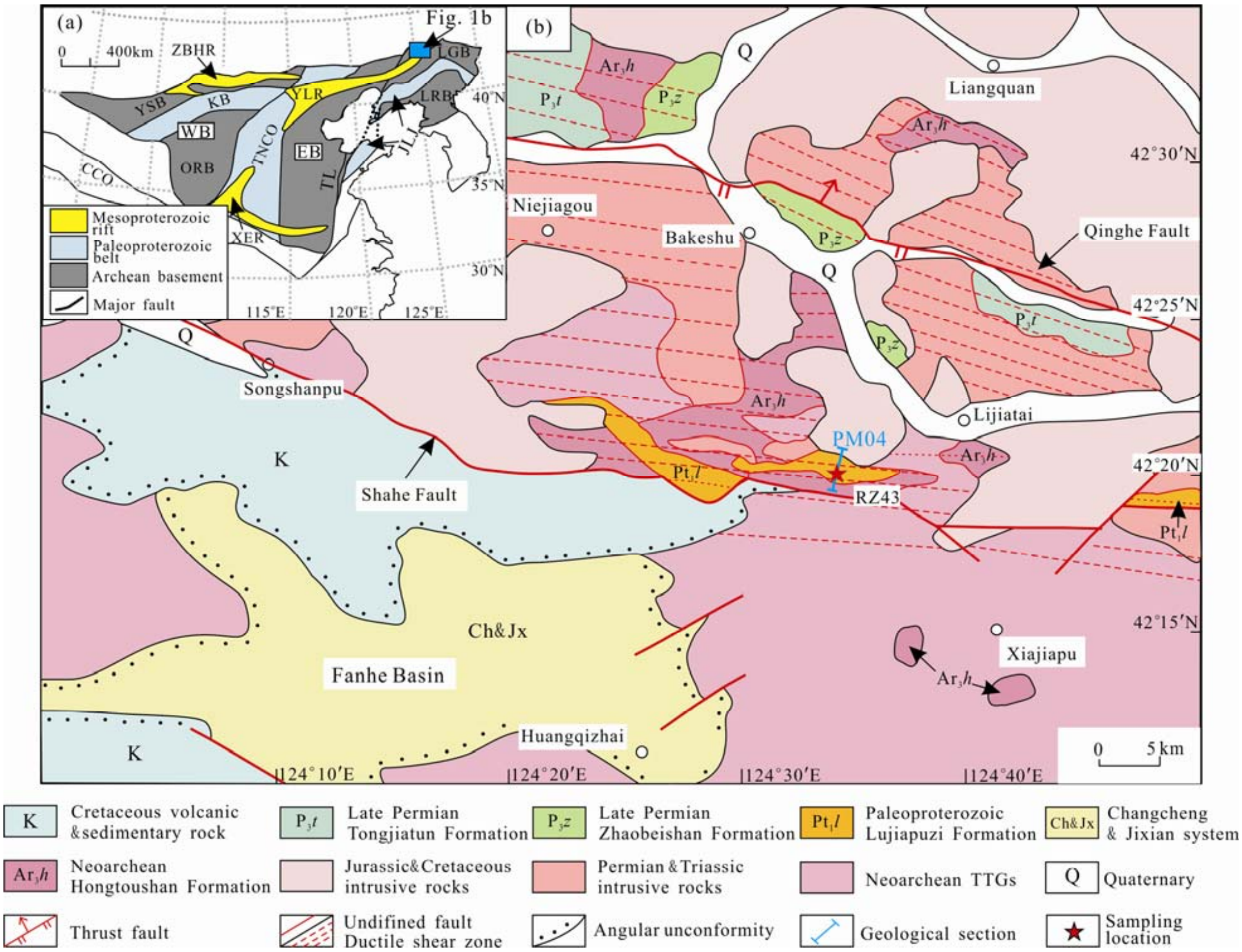

Fig. 1. Maps showing (a) the tectonic elements of the North China Craton (modified after Zhai Mingguo, 2004 and Zhao et al., 2005) and (b) the geology of study area (modified after Liu et al., 2017d), including sample locations.
WB: Western Block; EB: Eastern Block; LGB: LongGang Block; LRB: Langrim Block; YSB: YinShan Block; ORB: Ordos Block; KB: Khondalite Belt; TNCO: Trans-North China Orogen; CCO: Central China Orogen; JLJ: Jiao–Liao–Ji Belt; TL: Tan–Lu Fault; YLR: Yan–Liao rift; XRF: Xiong'er rift; ZBHR: Zha'ertai–Bayan Obo–Huade rift.

Paleoproterozoic to Mesoproterozoic sedimentary units have been divided into the Changcheng system (1.8–1.6 Ga), the Jixian system (1.6–1.4 Ga), and the Await name system (1.4–1.0 Ga) (Gao Linzhi et al., 2008; Lu et al., 2008; Li et al., 2013; Zhai et al., 2015). However, the age of the base of the Changcheng System remains controversial, with some authors suggesting an age of 1.8 Ga (Wan et al., 2003, 2006; Lu et al., 2008; Qiao Xiufu and Wang Yanbin, 2014; Zhai et al., 2015), whereas others favour an age younger than 1.7 Ga (He Zhengjun et al., 2011; Li Huaikun et al., 2011; Li et al., 2013; Zhang Jian et al., 2015).

Previous studies focussed on the Yanshan area within the western and central sections of the Yan-Liao Rift, but few have investigated the northeastern segment, especially the Fanhe area in the North Liaoning region. Furthermore, no accurate age data have been reported for the late Paleoproterozoic to Mesoproterozoic sedimentary rocks in this area. A suite of low-grade metasediments, known as the Lujiapuzi Formation, crops out along the northeastern margin of the NCC (Chen Yuejun et al., 2006). A lack of accurate age data means that the timing of formation of these rocks is debated. Furthermore, the relationship between these low-grade metamorphic rocks and the sediments in the Fanhe Basin is yet to be investigated.

Here we present new geochemical data, U-Pb detrital zircon ages, and Hf isotopic compositions for the Lujiapuzi Formation in order to constrain the timing of deposition, determine the provenance of the formation, and perform a regional stratigraphic correlation. This study also provides new constraints on the age of the base of the Changcheng System and the timing of crustal growth within the Eastern Block of the NCC.

2 Geological Background

The study area is located at the northeastern margin of the NCC, adjacent to the Fanhe Basin, which lies within the Yan-Liao Rift (Fig. 1a). The Qinghe (QHF) and Shahe faults (SHF) transect the study area and formed in the Early–Middle Triassic (Liu Jin et al., 2016; Liu et al., 2017d). The region to the south of the SHF belongs to the NCC, and mainly develop the Neoarchean Hongtoushan Formation and tonalite–trondhjemite–granodiorite (TTG) units (Fig. 1b). The Neoarchean rocks are overlain by the Changcheng and Jixian groups (Fig. 1b), which represent the major components of the Fanhe Basin. Compared with the Yanshan region, the Changcheng Group in the Fanhe Basin lacks the lower Changzhougou and Chuanlinggou formations, and instead comprises only the upper Tuanshanzi and Dahongyu formations (LBGMR, 2015). However, similar to the Yanshan region, the Jixian Group of the Fanhe Basin can be divided into the Gaoyuzhuang, Yangzhuang, Wumishan, Hongshuizhuang, and Tieling formations. The Changcheng and Jixian groups are characterized by a gradational change from siliciclastic to carbonate sediments during the period of deposition. In the Cretaceous, volcano-sedimentary units, dominated by terrigenous clastics and intermediate–acidic volcanic rocks, were deposited along the SHF (Fig. 1b).

The area between the QHF and SHF marks the tectonic boundary between the NCC and the Central Asian Orogenic Belt (CAOB) (Liu Jin, 2017; Liu et al., 2017d). In this area, units deposited in the Triassic or earlier commonly show evidence of intense ductile deformation, whereas rocks from the Jurassic and onwards lack such features. The geology of the area is complex, and comprises a mixture of tectonic slivers from the NCC and CAOB, together interpreted as a tectonic mélange (Liu Jin, 2017). The tectonic slivers comprise primarily Neoarchean NCC basement, late Permian CAOB meta-volcanic sediments, Permian-Triassic CAOB intrusive rocks, and a suite of intensely deformed low-grade metasediments (i.e. Lujiapuzi Formation; Fig. 1b). The northern end of the QHF contains widespread Jurassic-Cretaceous batholiths and stocks (Fig. 1b). Pre-Jurassic geological units in the northern side of the QHF are preserved mainly as xenoliths. However, these xenoliths rarely contain NCC material, indicating that the region may lie within the CAOB.

3 Field Investigations and Petrography

The Lujiapuzi Formation crops out sporadically within the SHF, which is relatively well exposed in the Shimengou area. To reveal the details of the lithologies and characteristics of the sedimentary sequence, we constructed a 1:2000 scale geological cross-section (PM04) (Fig. 2). The units in the region dip predominantly toward the N/NE. At the northern end of the cross-section, the sedimentary units are intruded by Jurassic diorites, whereas in the south, Neoarchean amphibolites have been thrust over carbonaceous slates (Fig. 2). The cross-section shows that the Lujiapuzi Formation has characteristics typical of sedimentary rocks, such as clear, rhythmic layering (Fig. 2). The lower section of the Lujiapuzi Formation comprises dominantly argillaceous and carbonaceous slates, whereas the upper section is dominated by interbedded quartzites and marbles (Fig. 2). During the late Permian orogenic event (Liu et al., 2017d), these units underwent ductile deformation that resulted in the formation of irregular folds in the marbles (Fig. 2). Such deformation did not affect the equivalent units within the Fanhe Basin. Previous studies have shown that the dominant lithologies of the Lujiapuzi Formation are quartzites, marbles, and slates, and their detailed petrographic features are described below.

Quartzites display a granoblastic texture and comprise quartz (<90%) with minor plagioclase and tremolite (<10%) (Fig. 3a), although the tremolite is locally enriched in some samples (~20%, Fig. 3b). Quartz grains are 0.1–0.5 mm in size and show a xenomorphic–granular texture with a weak preferred orientation of grains. Tremolite is fibrous and colourless, and displays medium–positive relief and second-order blue–green interference colours. Weak metamorphism is recorded by local gradations into metamorphic quartz sandstone. However, the metamorphosed samples are blastopsammitic, and evidence for siliceous cementation is preserved.

The tremolite–dolomite marbles are grey–white, display a prismatic granoblastic texture, and comprise mainly dolomite, tremolite, and minor diopside (Fig. 3c), with modal abundances of ~55%, ~40%, and ~5%, respectively. Dolomite is 0.1–0.4 mm in size, colourless under plane-polarized light, and displays high-order interference colours. Tremolite is 0.1–0.8 mm in size, thready and colourless, and shows moderate positive relief and second-order blue–green interference colours.

The slates are dominantly located at the base of the formation, and are partially intercalated with quartzites. They are dominated by argillaceous and carbonaceous slates that display a blastopelitic texture and contain a slaty cleavage. The slates comprise clay minerals (50%–60%) and quartz (20%–30%), with minor biotite and sericite (argillaceous slate) or carbonaceous material (carbonaceous slate) (Fig. 3d), all of which are aligned along the cleavage.

4 Analytical Methods and Samples

4.1 Whole-rock geochemical analyses

Two marble samples (PM04-1 and PM04-3), one

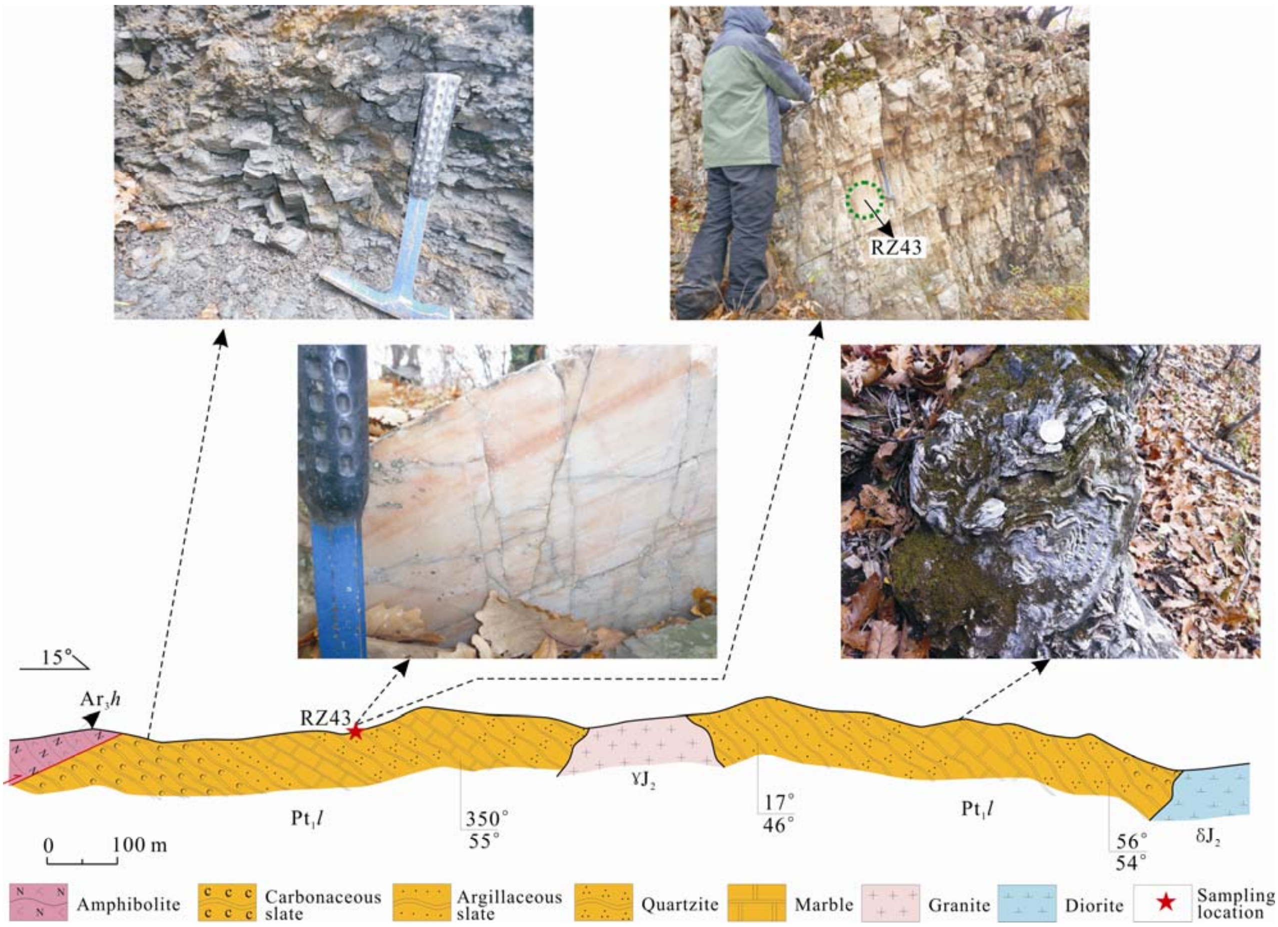

Fig. 2. Geological cross-section (PM04) and field photographs of the Lujiapuzi Formation.

quartzite sample (PM04-2) and two slate samples (PM04-4 and PM04-5) were analyzed during this study. Prior to analysis, weathered rims were removed and the samples were crushed to millimeter-size chips prior to handpicking under a binocular microscope. Fresh rock chips were selected and washed in an ultrasonic bath before being crushed to <200 mesh in a tungsten carbide jaw crusher. A split of this sample was ground to <200 mesh in an agate ring mill, and this material was used for major and trace element analyses.

All analyses were undertaken at the Shenyang Mineral Resources Supervision and Inspection Center, Shenyang, China. Whole-rock major element concentrations were determined by X-ray fluorescence spectrometry (XRF), yielding an analytical precision better than 2%. Trace element and rare earth element (REE) concentrations were determined by ICP-MS, following Qi et al. (2000) and yielding an analytical precision better than 5% for elements with concentrations of >10 ppm, <8% for elements with concentrations of <10 ppm, and ~10% for the transition metals. The major, trace, and REE compositions of these samples are given in Table 1.

4.2 Zircon LA-ICP-MS U-Pb dating

The sample dated during this study (quartzite sample RZ43) was collected from the Lujiapuzi Formation within the northeastern margin of the NCC at 42°20′27″N, 124°33′50″E. The sample was fresh and free of weathering. Zircons were separated using conventional magnetic and density separation techniques before being hand-picked under a binocular microscope, mounted in epoxy resin, and polished to approximately half-thickness. Cathodoluminescence (CL) imaging was undertaken by Nanjing Hongchuang GeoAnalysis, Nanjing, China, to outline the internal structures of individual zircons and select sites for U-Pb dating.

The zircon U-Pb analysis was performed using laser ablation–inductively coupled plasma–mass spectrometry (LA-ICP-MS) at Beijing Zhongshi Geological Analysis Laboratories, Beijing, China. The operating conditions for the LA system and the ICP-MS instrument, and data-reduction techniques were identical to those outlined by Liu et al. (2010), and are summarized here. The analyses were performed using a GeoLas 2005 laser (laser diameter 30 mm) attached to an Agilent 7500 ICP-MS instrument. Helium was used as a carrier gas and was mixed with

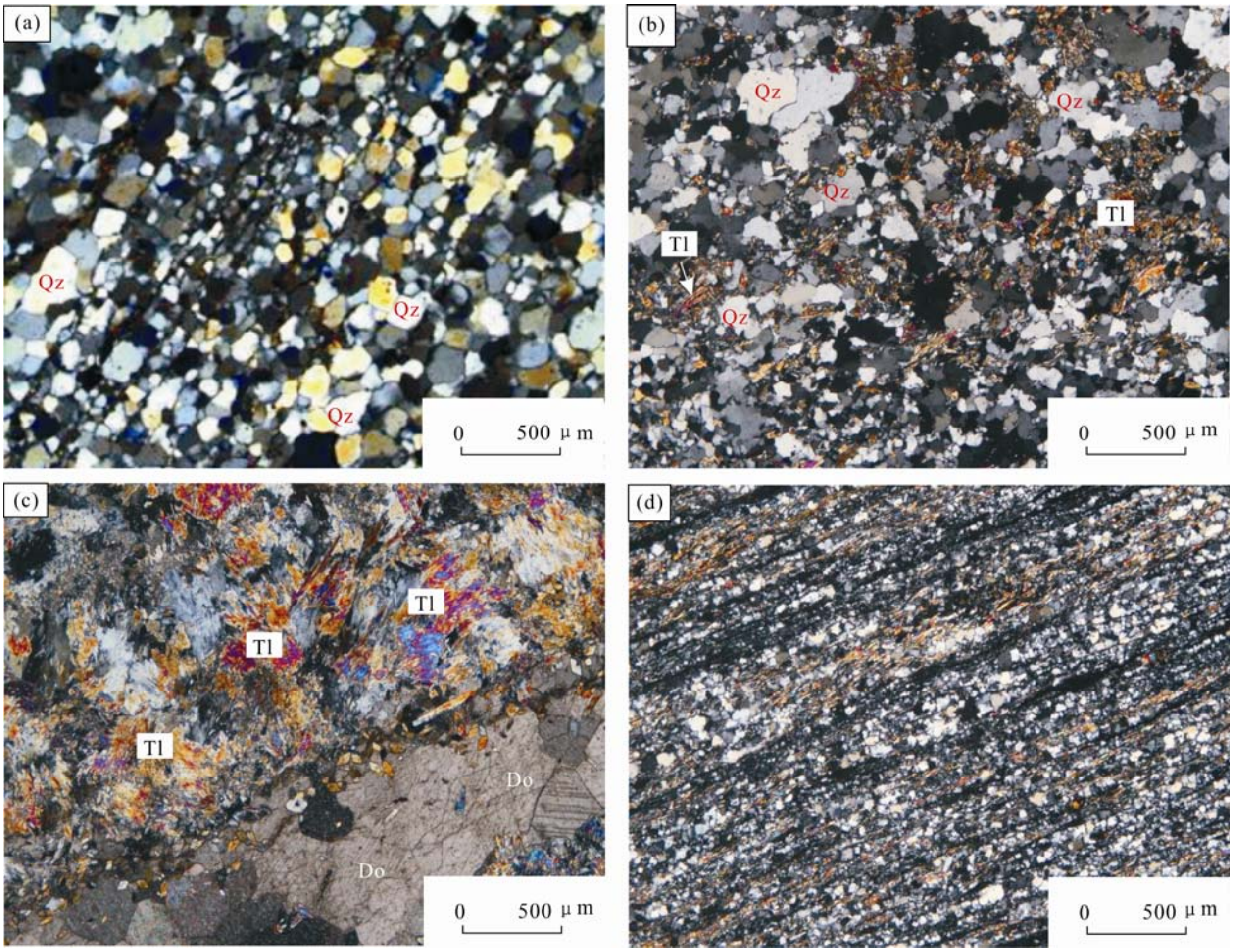

Fig. 3. Photomicrographs of representative samples of the Lujiapuzi Formation in the study area.
(a) Quartzite (cross-polarized light). (b) Tremolite quartzite (cross-polarized light). (d) Tremolite–dolomite marble (cross-polarized light). (e) Carbonaceous slate (cross-polarized light). Do: dolomite; Tl: tremolite; Qz: quartz.

Table 1 Major and trace concentrations of samples from the study area

Sample	Rocks type	SiO_2	Al_2O_3	Fe_2O_3	FeO	MnO	MgO	CaO	Na_2O	K_2O	TiO_2	P_2O_5	LOI
PM04-1	dolomite marble	0.80	0.90	0.95	0.23	0.15	16.27	40.40	0.05	0.07	0.03	0.02	37.82
PM04-2	quartzite	94.72	1.05	0.35	0.39	0.03	0.99	1.31	0.06	0.33	0.05	0.03	0.42
PM04-3	tremolite dolomite marble	31.94	1.05	0.27	0.45	0.08	16.17	27.48	0.09	0.42	0.06	0.04	21.22
PM04-4	carbonaceous slate	65.66	14.73	2.86	0.84	0.08	2.99	1.19	1.30	4.69	0.58	0.11	4.16
PM04-9	argillaceous slate	66.46	15.75	1.39	2.96	0.06	1.81	2.01	3.68	3.15	0.50	0.13	0.81

Sample	Rocks type	La	Ce	Pr	Nd	Sm	Eu	Gd	Tb	Dy	Ho	Er	Tm
PM04-1	dolomite marble	2.95	54.5	0.84	3.27	0.72	0.30	1.08	0.07	0.66	0.08	0.64	0.04
PM04-2	quartzite	5.80	5.1	1.24	4.90	1.03	0.30	0.75	0.11	0.86	0.17	0.45	0.08
PM04-3	Tremolite dolomite marble	6.19	64.3	1.16	4.17	0.78	0.33	0.90	0.09	0.56	0.12	0.62	0.06
PM04-4	carbonaceous slate	42.10	100.0	8.78	31.80	5.59	1.14	4.80	0.66	4.31	0.86	2.59	0.38
PM04-9	argillaceous slate	23.30	46.3	5.05	18.00	2.93	1.09	2.47	0.28	1.72	0.36	0.95	0.17

Sample	Rocks type	Yb	Lu	Y	ΣREE	LREE/ HREE	$(La/Yb)_N$	Eu_N/Eu_N^*	Ce_N/Ce_N^*	Nb	Ga	Zr	Th
PM04-1	dolomite marble	0.31	0.03	4.49	65.49	21.52	6.83	1.04	8.37	2.85	2.80	98.6	1.47
PM04-2	quartzite	0.32	0.06	8.80	21.10	6.55	13.00	1.00	0.44	2.66	2.21	142.0	1.58
PM04-3	tremolite dolomite marble	0.33	0.03	2.61	79.64	28.43	13.45	1.20	5.48	2.63	2.89	75.9	1.98
PM04-4	carbonaceous slate	2.73	0.41	33.10	206.15	11.31	11.06	0.66	1.21	12.00	23.30	427.0	22.40
PM04-9	argillaceous slate	1.08	0.13	6.50	103.83	13.50	15.48	1.21	1.00	8.15	20.00	175.0	10.90

Sample	Rocks type	Sr	Ba	V	Co	Cr	Ni	Rb	Ta	U	Hf	Li	Be
PM04-1	dolomite marble	208	46	9.2	2.2	12.4	11.5	4.3	0.08	0.22	1.11	8.8	0.19
PM04-2	quartzite	29	64	6.2	2.9	37.9	5.1	5.9	0.12	0.35	2.17	2.8	0.12
PM04-3	tremolite dolomite marble	59	62	6.2	2.9	13.4	14.9	21.0	0.11	0.51	0.80	22.3	0.14
PM04-4	carbonaceous slate	109	980	87.7	6.5	67.4	8.9	181.0	1.47	6.26	11.90	18.9	2.51
PM04-9	argillaceous slate	332	1074	72.0	13.7	71.8	25.7	89.4	0.39	0.69	3.46	20.0	0.95

Major elements are reported in wt%; trace and REE concentrations are reported in ppm. $Eu_N/Eu_N^*=2\times(Eu/0.0735)/((Sm/0.195)+(Gd/0.259))$; $Ce_N/Ce_N^*=2\times(Ce/0.808)/((La/0.310)+(Pr/0.122))$; $La_N/Yb_N=(La/0.310)/(Yb/0.209)$.

argon before entering the ICP unit. Nitrogen was added to the Ar plasma to decrease detection limits and improve precision (Hu et al., 2008). Each analysis consisted of a background acquisition of 20–30 s (gas blank) followed by 50 s of sample data acquisition. An Agilent Chemstation was used for data acquisition, off-line selection and integration of background and sample signals, and time-drift corrections. Quantitative calibrations were undertaken using ICPMSDataCal software (Liu et al., 2008, 2010). A 91500 standard zircon was used for external standardization of U/Pb ratios. All data were processed using Isoplot software (Ludwig, 2003).

4.3 Zircon Hf isotope

In situ zircon Hf isotopic compositions were analyzed using the Neptune multi-collector ICP-MS equipped with a 193 nm laser at the Institute of Geology and Geophysics, Chinese Academy of Sciences, Beijing. During the analyses, a spot size of 60 μm with a laser repetition rate of 10 Hz at 100mJ was used. The detailed analytical procedure and correction for interferences are similar to those described by Wu et al. (2006). All of the Hf analysis spots were located in the same CL domain as closely as possible to the U-Pb analysis spots.

The $\varepsilon_{Hf}(t)$ values and depleted mantle model ages (T_{DM}) are calculated assuming $^{176}Lu/^{177}Hf$ and $^{176}Hf/^{177}Hf$ ratios for average chondrite and the depleted mantle at the present day to be 0.0332 and 0.282772 and 0.0384 and 0.28325, respectively (Blichert-Toft and Albarede, 1997; Griffin et al., 2000). The decay constant for ^{176}Lu as 1.865×10^{-11} year^{-1} was adopted to calculate initial $^{176}Hf/^{177}Hf$ ratios (Scherer et al., 2001). The crust model age (T_{DM}^{C}) quoted here assumes that the parent magma to the zircon was produced from average continental crust ($^{176}Lu/^{177}Hf$=0.015; Griffin et al., 2004) that was originally derived from a depleted mantle source.

5 Analytical Results

5.1 Major elements

We analysed two marble samples, which both yielded relatively high MgO concentrations of 16.17 and 16.27 wt%. However, the CaO and SiO_2 concentrations, and loss on ignition (LOI) values of the two samples are distinct. Sample PM04-1 contains 40.40 wt% CaO and 0.80 wt% SiO_2, with 37.82 wt% LOI (Table 1). In contrast, PM04-3 contains 27.48 wt% CaO and 31.94 wt% SiO_2, with 21.22 wt % LOI (Table 1). The high MgO and CaO concentrations and LOI values indicate that the samples are composed dominantly of dolomite, and the high SiO_2 content of sample PM04-3 indicates the presence of tremolite. Quartzite sample PM04-2 yielded a high SiO_2 concentration of 94.72 wt% (Table 1), which is consistent with a mineralogy dominated by quartz. The carbonaceous and argillaceous slates contain relatively high SiO_2 and Al_2O_3 concentrations (Table 1), indicating that they are composed mainly of clay minerals and quartz.

5.2 Trace elements

The marble samples yielded total rare earth element (ΣREE) concentrations of 65.49–79.64 ppm, weakly positive Eu (Eu_N/Eu_N*=1.04–1.20) values, pronounced positive Ce (Ce_N/Ce_N*=5.48–8.37) anomalies (Table 1), and relatively high La_N/Yb_N values (6.83–13.45), indicating significant fractionation of REE. The samples are relatively enriched in light REE (LREE) and depleted in heavy REE (HREE) (Fig. 4a). Almost all minor elements are present in concentrations lower than those in the upper continental crust. However, the samples are

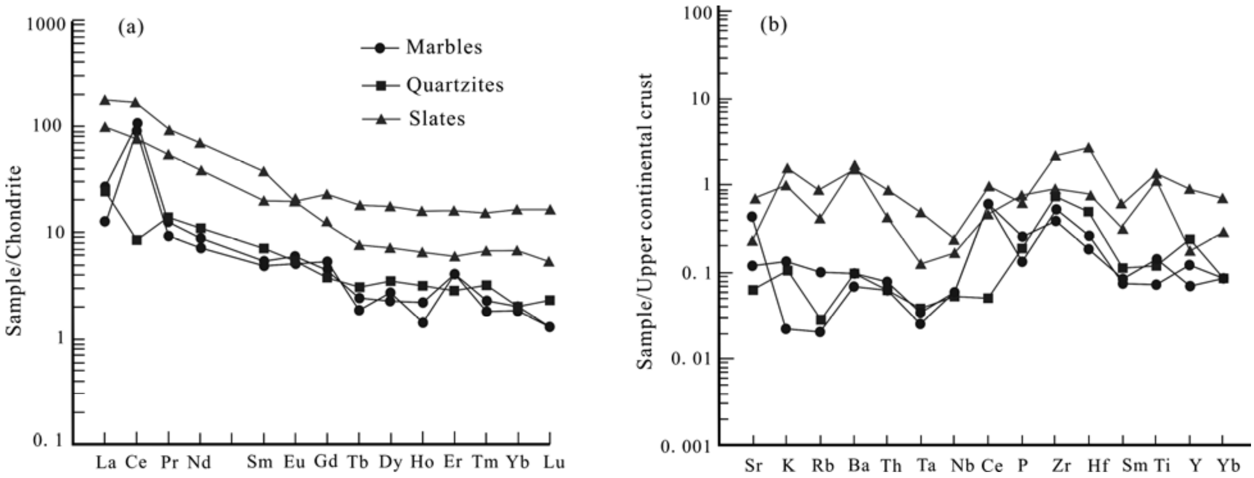

Fig. 4. (a) Chondrite-normalized REE concentrations and (b) upper-continental-crust-normalized multi-element variation diagram.

Chondrite normalization values are from Sun and McDonough (1989); upper-continental-crust normalization values are from Li Tong (1994).

relatively enriched in Ce, Zr, Hf, P, and Ti, and depleted in K, Rb, Ba, Th, Ta, and Nb (Fig. 4b).

The quartzite sample yields a low ΣREE value of 21.10 ppm, without Eu anomaly (Eu_N/Eu_N^*=1.00), but a clear negative Ce anomaly (Ce_N/Ce_N*=0.44) (Table 1), and shows relatively high La_N/Yb_N values (13.30). The sample is relatively enriched in LREE and depleted in HREE (Fig. 4a). Almost all minor elements are present in concentrations lower than those of the upper continental crust; however, the quartzite is relatively enriched in Zr, Hf, and Y (Fig. 4b), which may reflect zircon accumulation during transportation.

In contrast to the marble and quartzite samples, the carbonaceous and argillaceous slates yielded higher ΣREE values of 103.83–206.15 ppm, and Eu_N/Eu_N* values of 0.66 and 1.21, respectively. Unlike the marbles, Ce anomalies are not clear, with Ce_N/Ce_N* values of 1.21 and 1.00 for the carbonaceous and argillaceous slates, respectively. The slates yielded relatively high La_N/Yb_N values (11.06 and 15.48). Relative to the composition of the upper continental crust, the slate samples are enriched in K, Ba, Zr, Hf, and Ti, and relatively depleted in Ta, Nb, P, and Sm; other minor elemental concentrations are similar to those of the upper continental crust (Fig. 4b).

5.3 Zircon LA-ICP-MS U-Pb dating

Results of zircon U-Pb analysis are listed in Table 2, and CL images and concordia diagrams are shown in Figs. 5 and 6, respectively. Zircon grains are typically 50–200 μm in size, with aspect ratios of 1.0–2.0. The grains were rounded during transportation, and mainly display concentric oscillatory zoning in CL images (Fig. 5), and their Th/U ratios are mainly ＞0.4 (Table 2), indicative of a magmatic origin. By contrast, some zircons (e.g. analysis 4, 33, 36, and 79) show planar zoning or unzoned (Fig. 5), and their Th/U ratios are ＜0.4 (Table 2), indicative of a metamorphic origin.

A total of 92 LA–ICP–MS analyses yielded variable ages. A total of 64 concordant analyses (concordance > 90%) yielded ages from 2908 to 1746 Ma (Table 2), with most clustered within four age populations (Fig. 6b): 1791–1746 Ma (n=9), 2226–1803 Ma (n=38), 2398–2303 Ma (n=4), and 2576–2472 Ma (n=9). Three other grains yielded the oldest ages of 2706, 2713, and 2908 Ma (Table 2). The age group of 1791–1746 Ma yield U concentrations of 154.33–475.67 ppm, Th concentrations of 37.02–366.76 ppm, and Th/U ratios of 0.17–0.98 (see Table 2 for the data for each age group). The age group of 2226–1803 Ma yield U concentrations of 96.87–360.44 ppm, Th concentrations of 28.84–245.28 ppm, and Th/U ratios of 0.10–1.32. The age group of 2398–2303 Ma yield U concentrations of 171.38–288.77 ppm, Th concentrations of 64.52–256.35 ppm, and Th/U ratios of 0.26–1.22. The age group of 2576–2472 Ma yield U concentrations of 71.43–297.66 ppm, Th concentrations of 50.19–301.18 ppm, and Th/U ratios of 0.33–1.01.

5.4 Zircon Hf dating

Thirty zircon grains with concordant U–Pb ages from different age populations were analysed for their Lu–Hf isotopic compositions. The zircon grains with ages of 2713 and 2908 Ma have $\varepsilon_{Hf}(t)$ values of –6.2 and –2.4, and T_{DM2} model ages of 3.54 and 3.46 Ga (Table 3), respectively. The zircon grains with ages of 2706–2487 Ma yielded similar compositions ($^{176}Hf/^{177}Hf$=0.281190–0.281329, $^{176}Lu/^{177}Hf$=0.000295–0.000944, and $^{176}Yb/^{177}Hf$ = 0.010689–0.039202), they have $\varepsilon_{Hf}(t)$ values of +1.4 to +4.9, and T_{DM2} model ages of 2.94–2.74 Ga (Table 3). The zircons of 2398–1856 Ma have similar compositions ($^{176}Hf/^{177}Hf$=0.281188–0.281581, $^{176}Lu/^{177}Hf$=0.000018–0.001181, and $^{176}Yb/^{177}Hf$=0.000822–0.048320), their $\varepsilon_{Hf}(t)$ values and T_{DM2} model ages are –6.7 to –1.4 and 3.17 to 2.62 Ga, respectively (Table 3). The youngest zircon group (1789–1761 Ma) yielded similar compositions ($^{176}Hf/^{177}Hf$=0.281494–0.281663, $^{176}Lu/^{177}Hf$=0.000727–0.001371, and $^{176}Yb/^{177}Hf$=0.028190–0.056430), they have $\varepsilon_{Hf}(t)$ values of –6.5 to –0.5, and T_{DM2} model ages of 2.84 to 2.48 Ga (Table 3).

6 Discussions

6.1 Depositional age

The low-grade metasedimentary rocks exposed along the SHF were previously thought to have formed in the Paleoproterozoic, and were assigned to the Dashiqiao Formation of the Liaohe Group based on correlation of the regional stratigraphy (LBGMR, 1976). In contrast, Wang Dongfang et al. (1988) suggested that they represent a component of Early Cambrian ophiolitic mélange of the Qinghezhen Group. Subsequent 1:50,000 geological mapping assigned these rocks to the Neoarchean Banshigou Formation (LBGMR, 1993), whereas Chen Yuejun et al. (2006) regarded them as a component of the Paleoproterozoic Lujiapuzi Formation. More recent mapping during the Bakeshu and Dagujia Regional Geology Investigation Project identified a tectonic mélange within the QHF containing rocks with varying ages and affinities (Liu Jin, 2017), and assigned these low-grade metasedimentary rocks to the mélange. However, no accurate age data have been reported for these rocks.

Given that a sedimentary unit can be no older than its youngest detrital zircon grain (Gehrels, 2014), our youngest concordant $^{207}Pb/^{206}Pb$ age group with a weight mean age of 1780±9 Ma (late Paleoproterozoic), provides

Table 2 Results of the zircon LA–ICP–MS U–Pb analyses

Test No.	Total Pb	^{232}Th	^{238}U	Th/U	isotope ratio						isotopic age /Ma						concordance
	ppm	ppm	ppm		^{207}Pb/^{206}Pb	1σ	^{207}Pb/^{235}U	1σ	^{206}Pb/^{238}U	1σ	^{207}Pb/^{206}Pb	1σ	^{207}Pb/^{235}U	1σ	^{206}Pb/^{238}U	1σ	
1	84.88	52.34	126.16	0.41	0.1859	0.0016	13.4138	0.1345	0.5222	0.0041	2706	13	2709	9	2709	18	99%
2	37.99	52.26	83.19	0.63	0.1190	0.0012	5.8574	0.0627	0.3569	0.0028	1943	19	1955	9	1968	13	99%
3	113.97	63.90	310.78	0.21	0.1077	0.0008	4.7208	0.0410	0.3174	0.0022	1761	14	1771	7	1777	11	99%
4	117.96	37.82	297.24	0.13	0.1160	0.0008	5.5843	0.0475	0.3483	0.0024	1896	13	1914	7	1927	11	99%
5	114.87	247.42	385.29	0.64	0.1094	0.0008	3.5138	0.0297	0.2326	0.0014	1789	13	1530	7	1348	8	87%
6	93.56	122.95	139.21	0.88	0.1679	0.0012	11.0953	0.0965	0.4784	0.0033	2539	12	2531	8	2520	14	99%
7	59.13	64.60	93.83	0.69	0.1681	0.0014	11.1163	0.1178	0.4790	0.0042	2539	14	2533	10	2523	18	99%
8	126.42	132.94	674.41	0.20	0.1043	0.0008	2.3354	0.0184	0.1621	0.0009	1702	14	1223	6	969	5	76%
9	128.90	97.42	432.56	0.23	0.1088	0.0008	3.9047	0.0425	0.2596	0.0024	1780	13	1615	9	1488	12	91%
10	123.15	84.66	319.67	0.26	0.1159	0.0009	5.2116	0.0447	0.3254	0.0019	1894	15	1855	7	1816	9	97%
11	44.06	62.39	103.29	0.60	0.1136	0.0012	5.1994	0.0532	0.3324	0.0025	1858	18	1853	9	1850	12	99%
12	118.65	351.96	638.58	0.55	0.1171	0.0009	2.3747	0.0295	0.1468	0.0016	1922	14	1235	9	883	9	66%
13	63.91	46.38	126.88	0.37	0.1378	0.0011	7.7896	0.0747	0.4097	0.0032	2211	13	2207	9	2214	15	99%
14	82.09	104.42	183.18	0.57	0.1178	0.0009	5.7444	0.0550	0.3530	0.0025	1924	15	1938	8	1949	12	99%
16	153.58	193.94	545.71	0.36	0.1119	0.0007	3.7261	0.0305	0.2412	0.0017	1831	11	1577	7	1393	9	87%
17	64.76	82.83	95.04	0.87	0.1719	0.0013	11.6692	0.1149	0.4922	0.0040	2576	13	2578	9	2580	17	99%
18	115.71	120.95	193.32	0.63	0.1674	0.0012	10.4450	0.1005	0.4521	0.0037	2531	12	2475	9	2404	16	97%
19	141.61	207.72	453.90	0.46	0.1126	0.0008	3.9698	0.0317	0.2553	0.0016	1843	13	1628	6	1466	8	89%
20	129.81	92.36	595.05	0.16	0.1129	0.0009	3.0604	0.0402	0.1962	0.0022	1856	15	1423	10	1155	12	79%
21	110.94	99.11	174.43	0.57	0.1683	0.0012	11.2869	0.0961	0.4860	0.0034	2543	12	2547	8	2553	15	99%
22	160.62	174.71	284.47	0.61	0.1483	0.0010	8.8509	0.0707	0.4325	0.0029	2328	11	2323	7	2317	13	99%
23	224.83	488.49	1181.28	0.41	0.1072	0.0007	2.3156	0.0175	0.1565	0.0010	1752	13	1217	5	938	5	74%
24	103.42	107.62	265.89	0.40	0.1142	0.0008	5.1262	0.0517	0.3251	0.0027	1866	13	1840	9	1815	13	98%
25	102.28	127.08	250.59	0.51	0.1128	0.0008	5.1164	0.0379	0.3288	0.0020	1856	13	1839	6	1832	10	99%
27	82.43	115.62	192.20	0.60	0.1150	0.0009	5.4002	0.0480	0.3403	0.0024	1881	14	1885	8	1888	12	99%
28	98.16	98.03	257.19	0.38	0.1093	0.0008	4.8226	0.0440	0.3195	0.0024	1789	18	1789	8	1787	12	99%
29	195.17	350.38	636.02	0.55	0.1701	0.0015	5.6071	0.0531	0.2390	0.0016	2558	15	1917	8	1381	8	67%
30	107.39	108.57	309.72	0.35	0.1173	0.0009	4.7908	0.0450	0.2958	0.0022	1917	15	1783	8	1670	11	93%
31	166.51	160.08	209.40	0.76	0.2103	0.0014	16.6204	0.1482	0.5721	0.0043	2908	12	2913	9	2916	17	99%
32	109.31	148.19	294.04	0.50	0.1138	0.0008	4.8222	0.0415	0.3069	0.0021	1861	13	1789	7	1725	10	96%
33	97.38	1.60	236.39	0.01	0.1245	0.0009	6.4772	0.0541	0.3769	0.0026	2022	13	2043	7	2062	12	99%
34	50.56	67.40	122.45	0.55	0.1142	0.0010	5.2648	0.0583	0.3341	0.0029	1933	16	1863	9	1858	14	99%
35	133.34	235.63	659.24	0.36	0.1072	0.0008	2.5779	0.0204	0.1745	0.0012	1752	13	1294	6	1037	7	77%
36	77.09	37.02	212.54	0.17	0.1094	0.0008	4.8876	0.0458	0.3238	0.0023	1789	13	1800	8	1808	11	99%
37	164.30	256.35	288.77	0.89	0.1477	0.0010	8.4657	0.0618	0.4154	0.0024	2319	11	2282	7	2239	11	98%
39	122.58	123.15	427.45	0.29	0.1117	0.0008	3.7792	0.0332	0.2451	0.0017	1828	13	1588	7	1413	9	88%
40	104.16	108.53	168.86	0.64	0.1629	0.0013	10.5935	0.0961	0.4715	0.0036	2487	13	2488	8	2490	16	99%
42	63.17	74.11	150.56	0.49	0.1127	0.0009	5.3222	0.0507	0.3424	0.0027	1844	15	1872	8	1898	13	98%
43	91.13	99.52	221.16	0.45	0.1132	0.0008	5.2914	0.0475	0.3388	0.0027	1854	13	1867	8	1881	13	99%
44	72.86	57.51	220.15	0.26	0.1128	0.0009	4.4298	0.0399	0.2845	0.0019	1856	15	1718	7	1614	9	93%
45	57.31	47.34	146.33	0.32	0.1117	0.0009	5.1271	0.0476	0.3326	0.0024	1828	15	1841	8	1851	12	99%
46	114.57	315.88	443.63	0.71	0.1105	0.0008	3.0488	0.0308	0.1995	0.0017	1809	13	1420	8	1173	9	80%
47	162.32	182.57	767.41	0.24	0.1062	0.0007	2.7188	0.0328	0.1852	0.0020	1800	12	1334	9	1095	11	80%
48	163.09	298.44	813.41	0.37	0.0996	0.0007	2.3347	0.0250	0.1696	0.0015	1617	13	1223	8	1010	8	80%
49	69.96	35.82	166.93	0.21	0.1207	0.0009	5.9498	0.0486	0.3570	0.0023	1969	13	1969	7	1968	11	99%
50	61.40	65.02	138.61	0.47	0.1193	0.0010	5.9089	0.0594	0.3586	0.0029	1947	15	1963	9	1976	14	99%
51	77.77	77.95	194.43	0.40	0.1112	0.0009	5.0869	0.0522	0.3314	0.0028	1820	16	1834	9	1845	14	99%
52	114.92	206.82	349.76	0.59	0.1105	0.0008	3.9462	0.0311	0.2587	0.0017	1809	13	1623	6	1483	9	90%
54	57.12	110.78	132.98	0.83	0.1102	0.0010	4.9607	0.0583	0.3260	0.0029	1803	17	1813	10	1819	14	99%
55	112.32	84.57	161.81	0.52	0.1867	0.0012	13.5391	0.1114	0.5251	0.0036	2713	11	2718	8	2721	15	99%
56	129.42	48.41	336.86	0.14	0.1164	0.0008	5.3692	0.0372	0.3342	0.0019	1902	7	1880	6	1859	9	98%
57	123.96	86.71	592.10	0.15	0.1066	0.0008	2.6955	0.0218	0.1832	0.0012	1743	18	1327	6	1085	7	79%
58	89.54	144.37	247.93	0.58	0.1150	0.0009	4.5131	0.0429	0.2847	0.0023	1880	14	1733	8	1615	12	92%
59	110.89	208.75	171.38	1.22	0.1463	0.0010	8.7812	0.0755	0.4346	0.0029	2303	13	2316	8	2327	13	99%
60	50.18	66.07	96.87	0.68	0.1316	0.0012	7.1455	0.0731	0.3940	0.0030	2120	16	2130	9	2141	14	99%
61	98.27	28.84	207.89	0.14	0.1372	0.0010	7.7952	0.0814	0.4117	0.0035	2192	8	2208	9	2223	16	99%
62	123.91	282.43	360.04	0.78	0.1094	0.0008	3.9352	0.0340	0.2606	0.0017	1791	13	1621	7	1493	9	91%
63	132.63	366.76	372.64	0.98	0.1091	0.0008	3.9423	0.0341	0.2618	0.0018	1785	13	1622	7	1499	9	92%
64	148.52	201.71	610.54	0.33	0.1045	0.0007	3.0383	0.0328	0.2104	0.0019	1706	12	1417	8	1231	10	85%
65	146.35	344.62	523.73	0.66	0.1055	0.0007	3.1769	0.0271	0.2182	0.0015	1724	13	1452	7	1272	8	86%
66	115.13	133.95	457.72	0.29	0.1289	0.0009	3.8131	0.0284	0.2146	0.0012	2083	13	1596	6	1253	6	75%
67	204.55	812.27	673.17	1.21	0.1372	0.0009	4.4706	0.0475	0.2360	0.0022	2192	11	1726	9	1366	11	76%
68	172.56	344.71	584.26	0.59	0.1285	0.0013	4.1498	0.0493	0.2350	0.0026	2077	17	1664	10	1361	13	79%
69	107.65	176.11	253.87	0.69	0.1108	0.0009	5.0362	0.0473	0.3299	0.0025	1813	15	1825	8	1838	12	99%
70	82.17	213.90	162.04	1.32	0.1146	0.0010	5.4438	0.0554	0.3449	0.0028	1874	21	1892	9	1910	14	99%
71	172.60	301.18	297.66	1.01	0.1628	0.0012	9.2688	0.1074	0.4121	0.0040	2485	13	2365	11	2224	18	93%
72	133.06	363.25	654.13	0.56	0.0996	0.0007	2.2716	0.0193	0.1653	0.0011	1617	14	1204	6	986	6	80%
73	101.83	125.31	245.27	0.51	0.1127	0.0008	5.2425	0.0458	0.3369	0.0022	1844	13	1860	7	1872	11	99%
75	130.19	36.11	360.44	0.10	0.1139	0.0008	5.0890	0.0426	0.3241	0.0022	1862	13	1834	7	1810	11	98%
76	138.94	166.50	781.10	0.21	0.1049	0.0008	2.2680	0.0193	0.1568	0.0010	1722	14	1202	6	939	6	75%

Continued Table 2

Test No.	Total Pb ppm	^{232}Th ppm	^{238}U ppm	Th/U	isotope ratio ^{207}Pb/^{206}Pb	1σ	^{207}Pb/^{235}U	1σ	^{206}Pb/^{238}U	1σ	isotopic age /Ma ^{207}Pb/^{206}Pb	1σ	^{207}Pb/^{235}U	1σ	^{206}Pb/^{238}U	1σ	concor-dance
77	150.53	228.75	740.30	0.31	0.0993	0.0007	2.3801	0.0192	0.1738	0.0011	1611	13	1237	6	1033	6	82%
78	121.69	64.52	248.02	0.26	0.1547	0.0012	8.6388	0.0857	0.4048	0.0033	2398	12	2301	9	2191	15	95%
79	65.99	46.97	175.96	0.27	0.1087	0.0010	4.8359	0.0476	0.3224	0.0022	1789	16	1791	8	1802	11	99%
80	47.52	52.61	71.43	0.74	0.1663	0.0015	11.4238	0.1264	0.4982	0.0043	2521	15	2558	10	2606	18	98%
81	63.12	80.42	154.33	0.52	0.1068	0.0010	4.8374	0.0511	0.3283	0.0024	1746	17	1791	9	1830	12	97%
82	62.97	77.75	140.11	0.55	0.1206	0.0011	5.9389	0.0617	0.3576	0.0031	1965	16	1967	9	1971	15	99%
83	53.75	49.89	127.62	0.39	0.1186	0.0011	5.7592	0.0594	0.3522	0.0027	1936	16	1940	9	1945	13	99%
84	85.93	101.86	188.03	0.54	0.1221	0.0009	6.1085	0.0562	0.3626	0.0026	1987	47	1991	8	1994	12	99%
85	107.65	153.84	305.61	0.50	0.1183	0.0009	4.6534	0.0570	0.2848	0.0030	1931	13	1759	10	1615	15	91%
86	164.96	245.28	289.47	0.85	0.1399	0.0010	8.1252	0.0699	0.4208	0.0029	2226	13	2245	8	2264	13	99%
88	86.84	50.19	151.91	0.33	0.1614	0.0013	10.3744	0.0948	0.4660	0.0035	2472	13	2469	8	2466	16	99%
89	139.77	116.27	475.67	0.24	0.1088	0.0009	3.9160	0.0696	0.2592	0.0039	1781	15	1617	14	1486	20	91%
90	109.77	141.73	254.01	0.56	0.1304	0.0011	6.2042	0.0877	0.3438	0.0041	2103	15	2005	12	1905	20	94%
91	134.90	237.75	342.98	0.69	0.1295	0.0010	5.4383	0.0490	0.3043	0.0021	2091	14	1891	8	1712	10	90%
92	46.94	58.55	105.01	0.56	0.1185	0.0011	5.8785	0.0624	0.3595	0.0028	1944	17	1958	9	1980	13	98%

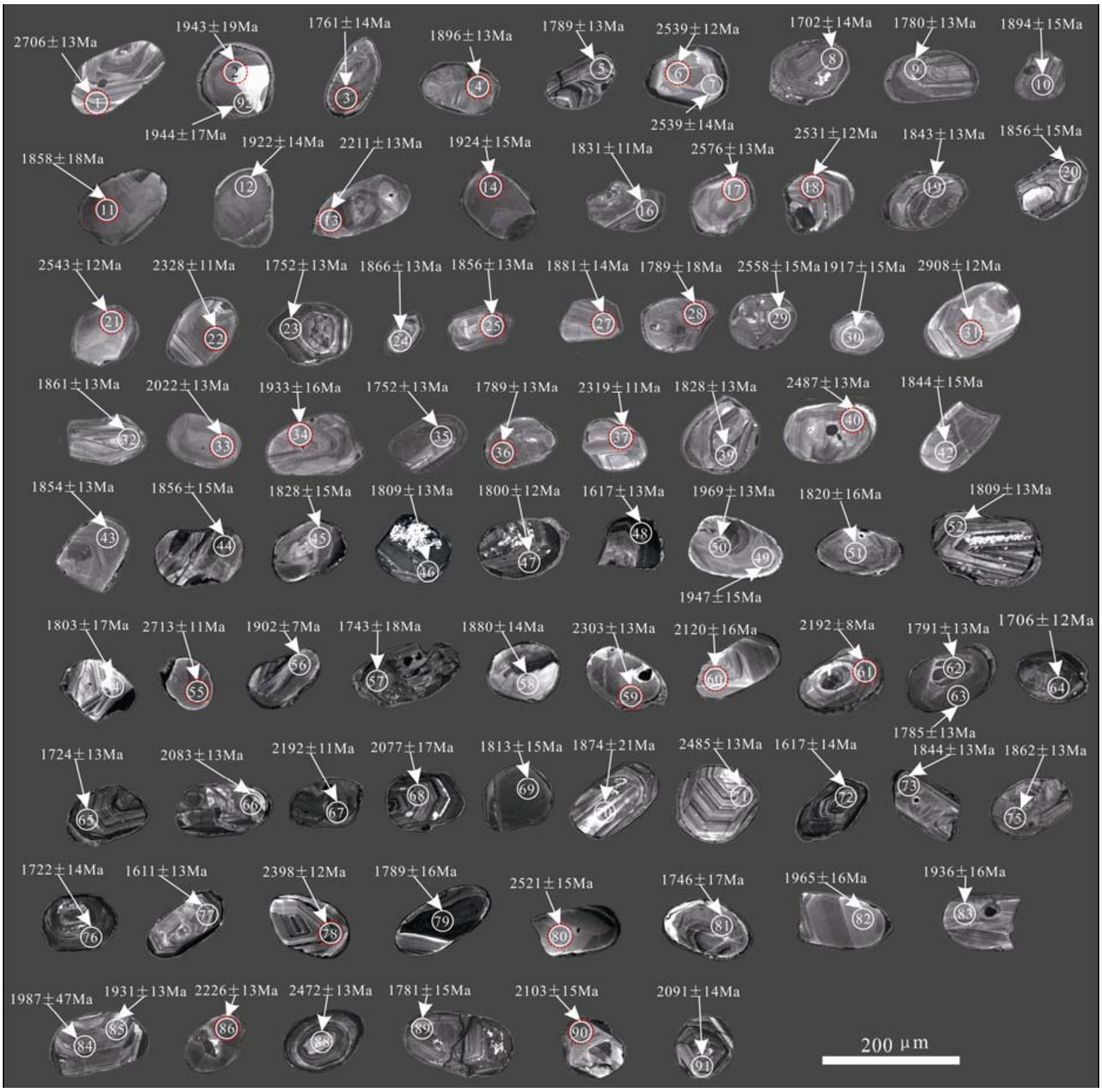

Fig. 5. Representative CL images of zircons from quartzite sample RZ43, showing the locations of spot analyses and the corresponding ^{206}Pb/^{207}Pb ages.

Table 3 In situ zircon Hf isotopic data for the RZ43.

Test No.	Age (Ma)	$^{176}Hf/^{177}Hf$	$^{176}Lu/^{177}Hf$	$^{176}Yb/^{177}Hf$	$\varepsilon Hf(0)$	$\varepsilon Hf(t)$	2σ	T_{DM1}	T_{DM2}	$f_{Lu/Hf}$
3	1761	0.281658	0.001185	0.047554	-39.4	-1.6	0.7	2246	2529	-0.96
90	1781	0.281494	0.000727	0.028190	-45.2	-6.5	0.8	2443	2843	-0.98
28	1789	0.281663	0.000897	0.036266	-39.2	-0.5	0.8	2223	2481	-0.97
36	1789	0.281568	0.001371	0.056430	-42.6	-4.4	0.6	2383	2724	-0.96
25	1856	0.281499	0.000701	0.029489	-45.0	-4.6	0.9	2434	2784	-0.98
11	1858	0.281474	0.000293	0.011716	-45.9	-4.9	0.7	2443	2806	-0.99
27	1881	0.281416	0.000537	0.022890	-48.0	-6.7	0.8	2536	2937	-0.98
4	1896	0.281581	0.001181	0.048320	-42.1	-1.4	0.7	2352	2618	-0.96
14	1924	0.281439	0.000180	0.007856	-47.1	-4.5	0.7	2482	2832	-0.99
34	1933	0.281490	0.000490	0.020253	-45.3	-2.9	0.7	2433	2739	-0.99
2	1943	0.281408	0.000018	0.000822	-48.3	-5.0	0.7	2514	2876	-1.00
33	2022	0.281340	0.000150	0.005850	-50.6	-5.8	0.7	2613	2983	-1.00
60	2120	0.281284	0.000995	0.041568	-52.6	-6.7	0.8	2747	3117	-0.97
61	2192	0.281453	0.000158	0.007463	-46.7	2.1	0.6	2462	2632	-1.00
13	2211	0.281402	0.000634	0.023325	-48.4	0.0	1.0	2562	2774	-0.98
86	2226	0.281301	0.000694	0.029202	-52.0	-3.3	0.7	2703	2991	-0.98
59	2303	0.281249	0.000936	0.038694	-53.9	-3.8	0.7	2790	3079	-0.97
37	2319	0.281283	0.001111	0.044802	-52.6	-2.5	0.7	2756	3012	-0.97
22	2328	0.281188	0.000657	0.027450	-56.0	-5.0	0.7	2852	3170	-0.98
78	2398	0.281295	0.000588	0.022111	-52.2	0.5	0.7	2703	2888	-0.98
40	2487	0.281291	0.000723	0.029160	-52.4	2.2	0.7	2718	2857	-0.98
80	2521	0.281243	0.000332	0.012661	-54.1	1.9	0.8	2755	2900	-0.99
18	2531	0.281238	0.000295	0.010689	-54.3	2.0	0.8	2759	2901	-0.99
6	2539	0.281248	0.000944	0.039202	-53.9	1.4	0.8	2791	2941	-0.97
21	2543	0.281329	0.000665	0.024437	-51.0	4.9	0.8	2663	2736	-0.98
17	2576	0.281259	0.000531	0.021064	-53.5	3.4	0.8	2747	2852	-0.98
1	2706	0.281190	0.000548	0.019385	-55.9	3.9	1.0	2841	2923	-0.98
55	2713	0.280891	0.000292	0.011747	-66.5	-6.2	0.8	3221	3537	-0.99
31	2908	0.280917	0.001136	0.050937	-65.6	-2.4	0.7	3256	3460	-0.97

a maximum age for the deposition of the Lujiapuzi Formation.

6.2 Determination of provenance

Dating of detrital zircon grains is an effective method for determining the provenance of sedimentary rocks (Wysoczanski et al., 1997; Geslin et al., 1999; Böhm et al., 2000; Cawood and Nemchin, 2000). Our quartzite sample (RZ43) yielded detrital zircon U–Pb ages of 2908–1746 Ma (Fig. 6; Table 2) that define four populations: 2576–2472 Ma (n=9), 2398–2303 Ma (n=4), 2226–1803 Ma (n=38), and 1791–1746 Ma (n=9). These ages record the timing of thermo-tectonic events that affected the source rocks of the Lujiapuzi Formation.

6.2.1 Zircons from Archean crystalline basement

Neoarchean crystalline basement is widely exposed along the northern margin of the NCC. Recently acquired zircon U-Pb ages indicate that the basement formed at ca. 2.5 Ga (Wan Yusheng et al., 2005; Zhai et al., 2005; Liu et al., 2011; Liu Jin et al., 2017; Wang et al., 2016a; Shi and Zhao, 2017; Song Jian et al., 2018). Therefore, the 2576–2472 Ma detrital zircon grains from the Lujiapuzi Formation were most likely derived from NCC crystalline basement.

The three zircon grains that yielded ages of 2908, 2713, and 2706 Ma were also likely derived from NCC basement. Liu et al. (2017c) reported a newly discovered Mesoarchean gneiss in northern Liaoning Province, which is dated at 2857±17 Ma. We infer that the 2908 Ma zircon grain was likely derived from this Mesoarchean gneiss. Currently, no ca. 2.7 Ga rocks have been reported in the Northern Liaoning region; however, abundant ca. 2.7 Ga rocks are observed in other areas of the NCC, indicating the existence of a widespread ca. 2.7 Ga crustal material within the NCC (Guan et al., 2002; Tang et al., 2007; Jahn et al., 2008; Wan et al., 2011a; Wang et al., 2017a). Some researchers suggest that early Neoarchean basement (ca. 2.7 Ga) may be more extensive than is currently recognised within the NCC, with the limited exposure resulting from intra-crustal reworking and overprinting by a tectonothermal event at ca. 2.5 Ga. (Jiang et al., 2010; Wan et al., 2011a; Wang et al., 2012). Therefore, the 2706 and 2713 Ma zircon grains suggest that ca. 2.7 Ga rocks occur within the Northern Liaoning area, as in other regions of the NCC, but have yet to be discovered.

6.2.2 Zircons related to Paleoproterozoic orogenic events

In the Paleoproterozoic, the NCC underwent a series of tectono-magmatic events. Therefore, detrital zircon grains with Paleoproterozoic ages are complex, and are divided into three populations (2398–2303, 2226–1803, and 1791–1746 Ma). The provenance of each of these groups is discussed below.

(1) 2398–2303 Ma zircons

There is little evidence for magmatism or metamorphism at ca. 2.4–2.3 Ga in the NCC or elsewhere on Earth (Condie et al., 2009; Wan et al., 2011b). Currently, no ca. 2.4–2.3 Ga magmatic rocks have been reported in the Northern Liaoning area or the Longgang Block. However, abundant ca. 2.4–2.3 Ga detrital zircons have been identified in the Paleoproterozoic Liaohe, Changcheng, and Mesoproterozoic Jixian groups (Ren Rong et al., 2011; Wan et al., 2011b; Duan Chao et al., 2014), suggesting that widespread magmatism occurred in the Northern Liaoning area or Longgang Block at this time. Therefore, the 2398–2303 Ma zircon grains may have been derived from these yet undiscovered ca. 2.4–2.3 Ga magmatic rocks. Furthermore, many ca. 2.4–2.3 Ga magmatic rocks have been observed along the western margin of the Eastern Block, in Western Henan province (Diwu Chunrong et al., 2007; Jiang Zongsheng et al., 2011; Huang Daomao et al., 2012; Huang et al., 2012), and in the Zhongtiaoshan (Zhao Fengqing et al., 2006) and Lüliang areas (Geng Yuansheng et al., 2006; Zhao et al., 2008; Zhao Jiao et al., 2015). The 2.4–2.3 Ga magmatism may therefore have occurred across an extensive area of the NCC, and early Paleoproterozoic magmatism may have been an important event during the evolution of the craton.

(2) 2226–1803 Ma zircons

Magmatic rocks that yield ages of ca. 2200–1800 Ma are widely exposed in the Liao-Ji Belt of the Eastern Block, and include the Liaoji granitoids (ca. 2.2–2.1 Ga; Lu Xiaoping et al., 2004a, b; Lu et al., 2006; Wan et al., 2006; Li and Zhao, 2007; Wang et al., 2017b; Liu et al., 2018), meta-volcanic rocks of the Li'eryu Formation (ca. 2.2–2.1 Ga; Sun et al., 1993; Wan et al., 2006; Li Zhuang et al., 2015; Chen Bin et al., 2016), the Haicheng mafic sills/dykes (ca. 2.2–2.1 Ga; Yu Jiejiang et al., 2007; Meng et al., 2014; Yuan et al., 2015; Wang et al., 2016b; Li et al., 2016), the Kuangdonggou syenite (ca. 1.87–1.85 Ga; Cai Jianhui et al., 2002; Yang Jinhui et al., 2007; Zhang Peng et al., 2016), the Qingchengzi granite (ca. 1.89 Ga; Wang et al., 2017b), and the Tonghua diorite–monzogranite–syenite complex (ca. 1.87–1.85 Ga; Lu Xiaoping et al., 2005; Liu et al., 2017b).Thus, these 2226–1803 Ma zircon grains were likely derived from Paleoproterozoic magmatic rocks of the Liao-Ji Belt, which represents the dominant source of the Lujiapuzi Formation. Therefore, Paleoproterozoic magmatic rocks of the Liao-Ji Belt must have been uplifted prior to the deposition of the Lujiapuzi Formation. This inference is consistent with suggestions by Zhai et al. (2000) and Guan et al. (2002) that the NCC was uplifted at 1.83–1.79 Ga.

(3) 1791–1746 Ma zircons

The Eastern and Western blocks collided along the TNCO at ca. 1.85 Ga. Following amalgamation, three major rift zones formed within the NCC or along its margins (i.e., the Xiong'er, Yan-Liao, and Zha'ertai–Bayan Obo rift zones; Zhai et al., 2000, 2015; Zhai Mingguo, 2004; Lu et al., 2008; Peng et al., 2011; Zhai and Santosh, 2011). Volcanic rocks within the Changcheng and Jixian systems of the Yan-Liao Rift are younger than ca. 1.70 Ga (Lu et al., 2002, 2008; Lu Songnian et al., 2003; Gao Linzhi et al., 2007, 2008; Hu Junliang et al., 2007; Su et al., 2008; Li Huaikun et al., 2009; Su Wenbo et al., 2010; Tian Hui et al., 2015; Wang et al., 2015; Zhang Jian et al., 2015). Peng et al. (2012) described the Miyun mafic dykes that formed at ca. 1.73 Ga, representing the only known ca. 1.80–1.70 Ga magmatic rocks in the Yan-Liao Rift. However, our 1791–1746 Ma zircon grains display concentric oscillatory zoning that is typical of moderate–acidic magmatic rocks (Fig. 5), which is inconsistent with being sourced from the Miyun mafic dykes.

Peng et al. (2008) proposed that the Xiong'er Rift contained a ca. 1.78 Ga volcanic province of mainly intermediate volcanic rocks with minor basalts (Zhao et al., 2002). Zhao et al. (2004) presented SHRIMP ages for the Xiong'er volcanic province that range from ca. 1.80 to 1.75 Ga, and Zhai et al. (2015) suggested that these volcanic rocks represent the earliest record of the Xiong'er Rift. However, the Xiong'er Rift and Fanhe Basin are separated by a considerable distance. Thus, it is more likely that the 1791–1746 Ma zircon grains were sourced from an undiscovered ca. 1.80–1.75 Ga magmatic unit that existed in the North Liaoning province, which was likely produced during the earliest magmatism in the Yan-Liao Rift.

In summary, the Archean basement of the Longgang Block and the Paleoproterozoic Liao-Ji Belt were the primary sources of the Lujiapuzi Formation (Fig. 7), which is dominated by 2.9–2.5 Ga and 2.3–1.8 Ga sediments.

6.3 Protolith determination and regional stratigraphic correlation

6.3.1 Protolith determination

Our field investigations indicate that the dolomitic marbles, quartzites, and argillaceous and carbonaceous slates of the Lujiapuzi Formation are systematically layered with a clear stratigraphy. In addition, blastobedding structures were observed in the quartzites. The marbles comprise dolomite and tremolite, indicating derivation from dolomitic protolith. The quartzites are dominated by quartzes and preserve rare blastopsammitic textures, consistent with quartz sandstone protolith. The argillaceous and carbonaceous slates are composed primarily of clay minerals and quartzes, indicating that their protolith were mudstones.

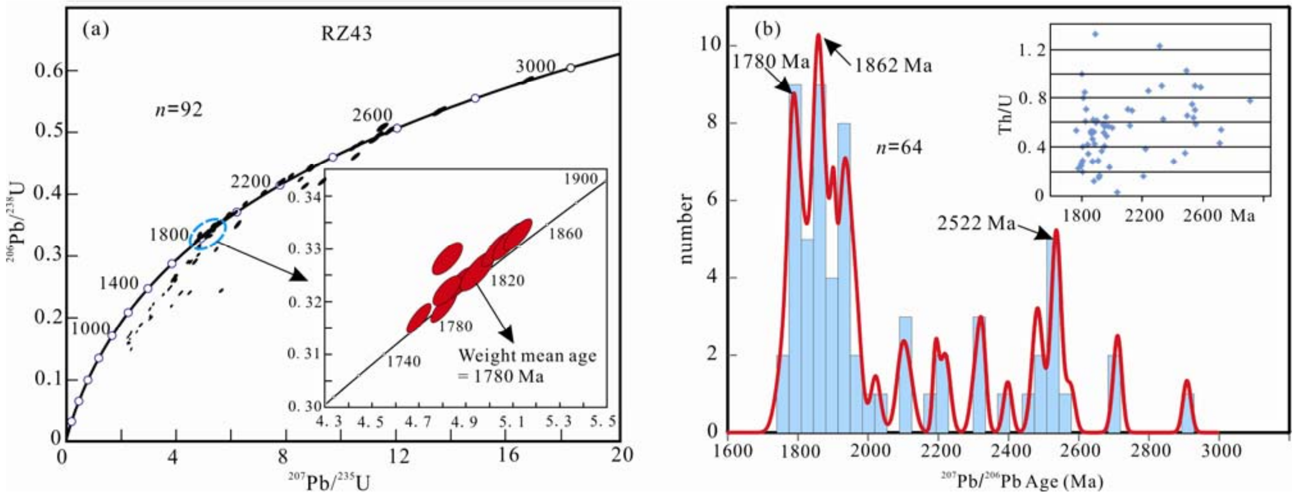

Fig. 6. (a) Concordia plot (concordance > 90%) and (b) $^{207}Pb/^{206}Pb$ age histogram showing the results of LA–ICP–MS U–Pb analyses on zircon grains from quartzite sample RZ43.

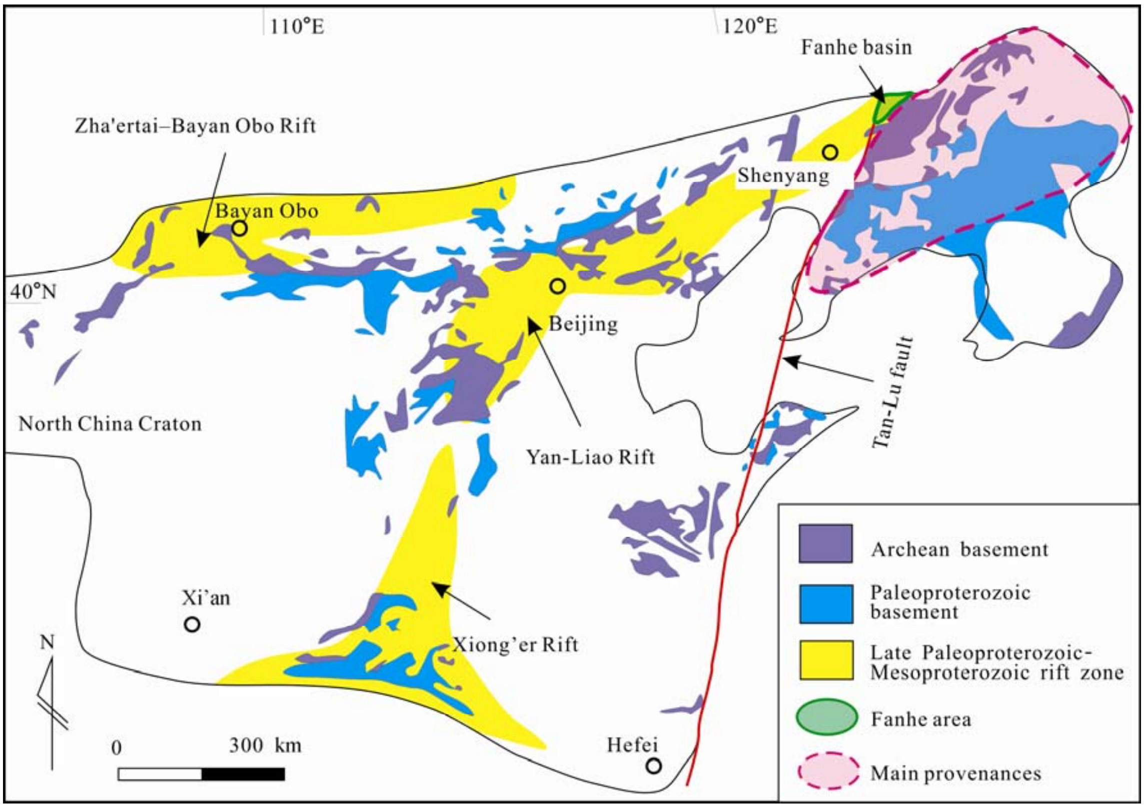

Fig. 7. Sketch map of possible sources for the Lujiapuzi Formation (modified from Liu et al., 2017a).

Geochemistry can be used to determine the protolith of metamorphic rocks, with the Si vs (al+fm) – (c+alk) and (La/Yb) vs ∑REE diagrams being commonly used (Simonen, 1953). On the (al+fm) – (c+alk) vs Si diagram (Fig. 8a), the marble, quartzite, and slate samples plot within the fields for calcareous sedimentary rocks, sandstone, and mudstone, respectively, whereas on the (La/Yb) vs ΣREE diagram (Fig. 8b) they plot within fields for carbonate, sandstone, greywacke, shale, and mudstone. In summary, mineral assemblages and compositions, and geochemical data all indicate that the protoliths of the Lujiapuzi Formation were dominantly dolomites, quartz sandstones, mudstones, and carbonaceous mudstones.

6.3.2 Regional stratigraphic correlation

The Lujiapuzi Formation initially comprised dolomites, quartz sandstones, mudstones, and carbonaceous mudstones, which now occur as tectonic slivers within the SHF. Ductile deformation and low-grade metamorphism that affected the formation were related to the collision

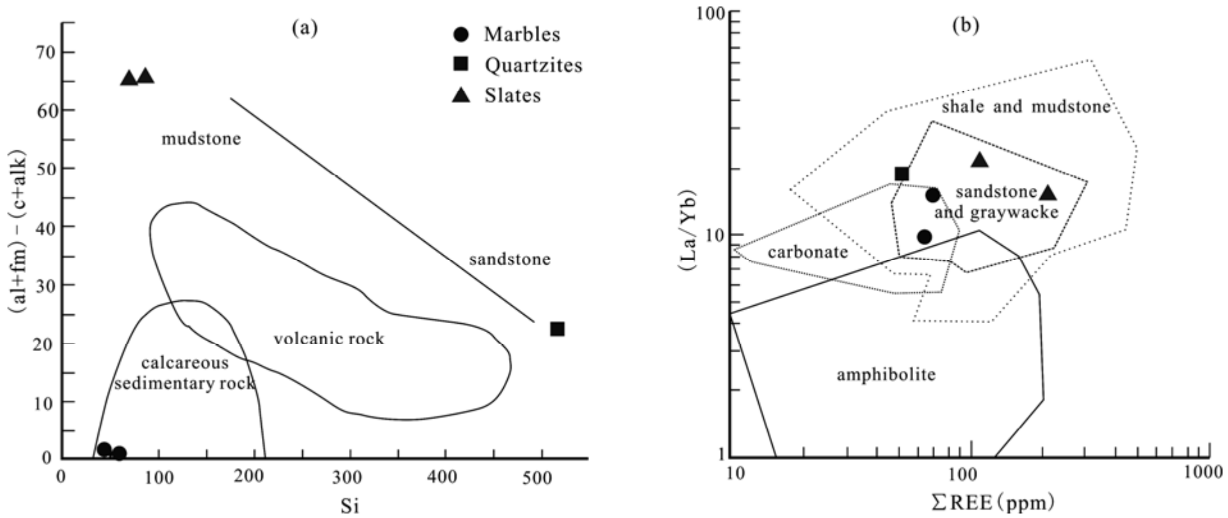

Fig. 8. (a), (al+fm)–(c+alk) vs Si diagram (after Simonen, 1953); (b), (La/Yb) vs ΣREE diagram (after Wang Renmin et al., 1987).
S=Al_2O_3+$2Fe_2O_3$+FeO+MgO+MnO+CaO+Na_2O+K_2O; al=(Al_2O_3/Σ)×100; fm=($2Fe_2O_3$+FeO+MgO+MnO)/Σ×100; c=(CaO/Σ)×100; alk=(Na_2O+K_2O)/Σ×100; al+fm+c+alk=100.

between the NCC and CAOB in the late Permian to Early Triassic (Liu et al., 2017d). The metasedimentary units of the Lujiapuzi Formation are adjacent to the Fanhe Basin (Fig. 1b), which is thought to represent the northeastern segment of the Yan-Liao Rift. Detrital zircon age characteristics of the metasedimentary rocks indicate that they correlate with the late Paleoproterozoic–Mesoproterozoic sedimentary cover in the Fanhe Basin (Figs. 6 and 9). Specifically, the upper section of the Lujiapuzi Formation comprises mainly quartzites intercalated with carbonaceous slates and is considered equivalent to the lower Dahongyu Formation (Fig. 9). The middle section contains marbles, quartzites, and intercalated carbonaceous slates, and is correlated with the Tuanshanzi Formation (Fig. 9). The lower section, which contains carbonaceous and argillaceous slates intercalated with quartzites, is equivalent to the upper Chuanlinggou Formation (Fig. 9). LBGMR (1988, 2015) proposed that the Fanhe Basin lacks the Changzhougou and Chuanlinggou formations of the lower Changcheng System. As the lower Lujiapuzi Formation is considered equivalent to the upper Chuanlinggou Formation, the lower Lujiapuzi Formation likely preserves the earliest deposited sediments of the Fanhe Basin.

In addition to the Lujiapuzi Formation, low-grade metamorphosed, strongly deformed sedimentary rocks have been observed along the eastern segment of the Chifeng-Kaiyuan fault of the NCC (NW Liaoning province). These rocks consist of the Cijiazhangzi and Weijiagou formations, the Taiheshen quartzites, and the Houxiaohuang marbles (LBGMR, 1988, 2015; Liu Zhenghong et al., 1999b, Liu Jin et al., 2013), which occur as tectonic slivers of marbles, quartzites, and various schists. Chen Yuejun et al. (2006) and LBGMR (2015) argued that these metasedimentary rocks are equivalent to the Paleoproterozoic Liaohe Group, and proposed a northern rift zone along the northern margin of the NCC; however, this model is not supported by precise age data. Zhao et al. (2012) showed that Paleoproterozoic rocks belonging to the TNCO (the Hongqingyingzi and Dantazi "groups or complexes") are exposed in northern Hebei province (Geng Yuansheng et al., 1997; Wang Renmin et al., 2002). These units record a regional high-pressure granulite-facies metamorphic event at 1.9–1.8 Ga (Mao Debao et al., 1999). In contrast, metasedimentary rocks in north-western Liaoning and the Lujiapuzi Formation underwent greenschist-facies metamorphism. Furthermore, Liu Zhenghong et al. (1999a, b) identified late Mesoproterozoic micro-plant fossil assemblages in the Weijiagou Formation, which are similar to those observed in the Changcheng and Jixian systems. In summary, we suggest that the Lujiapuzi Formation and the metasedimentary rocks along the northern fault of the NCC are related to the Yan-Liao Rift, rather than the TNCO or the ZBHR, and were metamorphosed and deformed during the late Permian orogenic event.

6.4 Tectonic implications

6.4.1 Age constraints on the base of the Changcheng System

The age of the base of the Changcheng System remains controversial, with some authors suggesting an age of 1.80 Ga (Wan et al., 2003; Lu et al., 2008; Qiao Xiufu and Wang Yanbin, 2014; Zhai et al., 2015) and others an age of <1.70 Ga (He Zhengjun et al., 2011; Li Kuaikun et al., 2011; Li et al., 2013; Zhang Jian et al., 2015). Wan et al.

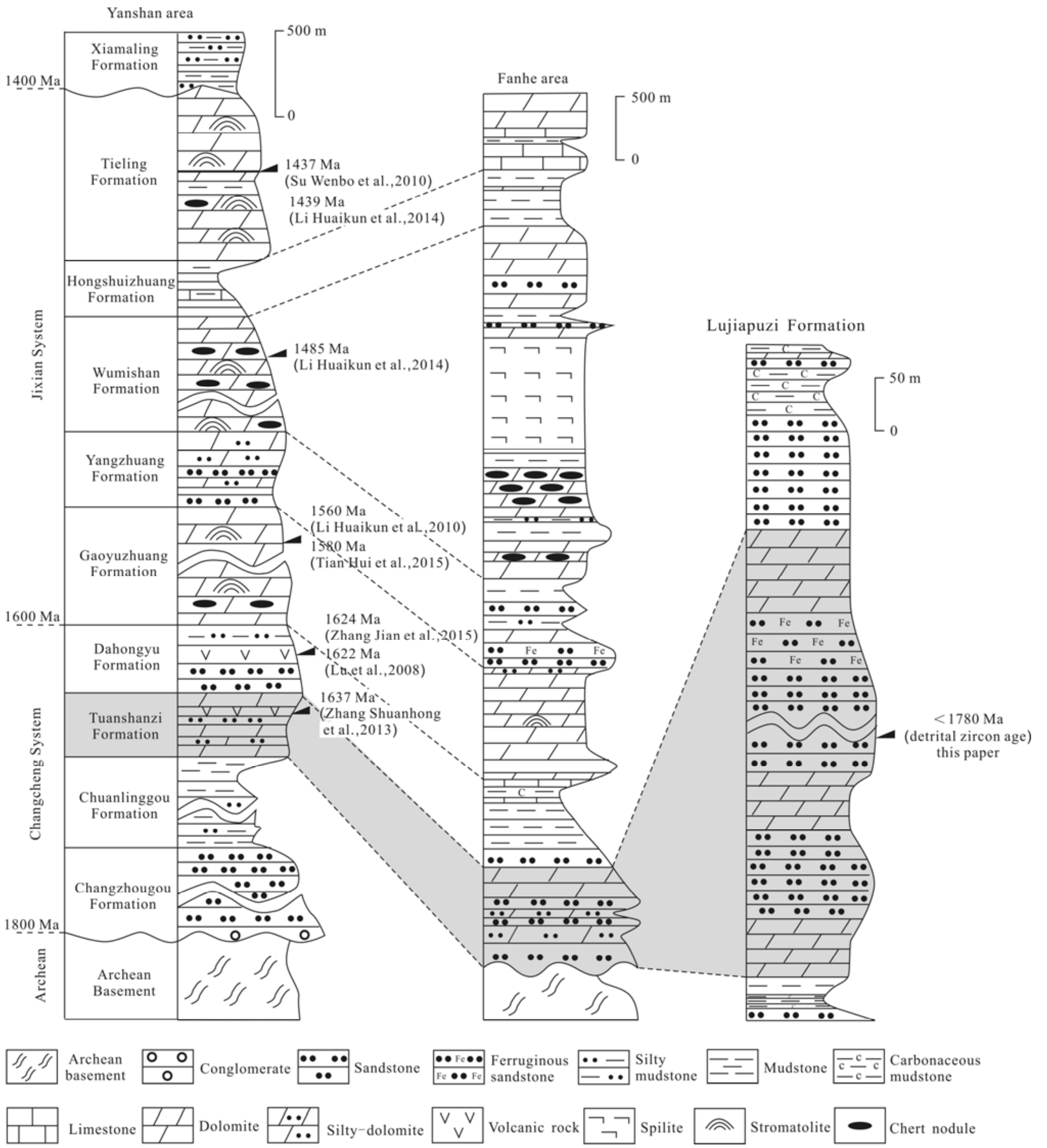

Fig. 9. Late Paleoproterozoic–Mesoproterozoic stratigraphic column for the Lujiapuzi area and correlation with the Yanshan and Fanhe areas.

The stratigraphic column for the Yanshan area is based on Su Wenbo et al. (2010) and ages are from Lu et al. (2008), Li Huaikun et al. (2010, 2014), Su Wenbo et al. (2010), Zhang Shuanhong et al. (2013), Zhang Jian et al. (2015) and Tian Hui et al. (2015). The stratigraphic column for the Fanhe area is based on LBGMR (2015).

(2003) reported SHRIMP U–Pb zircon detrital ages from an arkosic sandstone of the Changzhougou Formation and recognized several zircon populations, of which the youngest is ca. 1.80 Ga, indicating that deposition of the Changzhougou Formation occurred later than 1.80 Ga. Li et al. (2013) reported a zircon age of 1.67 Ga from a granitic vein that occurs within Archean gneiss and is unconformably covered by quartz sandstone of the Changzhougou Formation, and proposed that the age of the basal boundary is younger than 1.70 Ga. He Zhengjun et al. (2011) reported zircon ages of 1.71–1.68 Ga from the Rapakivi granite beneath the Changcheng System.

However, no consensus has been reached on the interpretation of these ages, and the previously described unconformity beneath the Changcheng System has been reinterpreted as a fault surface (Zhai et al., 2015). Zhao et al. (2004) reported magmatic zircon ages of ~1.78 Ma from the Xiong'er Formation, suggesting that the late Paleoproterozoic Xiong'er Rift developed earlier and may therefore record a more complete sedimentary succession than the Yan-Liao Rift. The Xiong'er Formation represents the lowermost unit of the late Paleoproterozoic sequences of the NCC, and the Ruyang Formation within the Xiong'er Rift has been correlated with the Changcheng System in the Yan-Liao Rift (Zhai et al., 2015).

Correlation with the regional stratigraphy indicates that the middle section of the Lujiapuzi Formation is equivalent to the Tuanshanzi Formation. Zhang Shuanhong et al. (2013) obtained an age of 1637±15 Ma from K-rich volcanic rocks within the upper Tuanshanzi Formation, and we can therefore further constrain the deposition age of the Lujiapuzi Formation to between ca. 1.78 and 1.64 Ga. The thick sedimentary units of the Changzhougou and Chuanlinggou formations were likely deposited over an extended period. We therefore infer that the age of the base of the Changzhougou Formation may be much older than the age of deposition of the Lujiapuzi Formation (1.78–1.64 Ga). Furthermore, as mentioned above, detrital zircons with ages of 1.80–1.75 Ga may represent the earliest rift-related magmatism in the Yan-Liao Rift. These constraints suggest that the base of the Changcheng System has an age of ca. 1.80 Ga.

6.4.2 Constraints on crustal growth along the north-eastern margin of the North China Craton

The high closure temperature of Hf in zircon reduces the influence of later magmatic processes or metamorphism, except for the formation of overgrowths (Kinny et al., 1991; Kinny and Maas, 2003). Thus, zircon Lu–Hf isotopic data can be used to determine magmatic sources and petrogenetic processes, and constrain the history of crustal growth (Wu Fuyuan et al., 2007).

The zircon grains with ages of 2713 and 2908 Ma have $\varepsilon_{Hf}(t)$ values of −6.2 and −2.4, and older T_{DM2} model ages of 3.54 and 3.46 Ga (Fig. 10a), suggesting that they crystallised from magmas generated during Paleoarchean crustal recycling. In contrast, zircon grains with ages of 2706–2487 Ma were most likely derived from basement gneisses (Wu et al., 2005, 2008). These Neoarchean zircons have $\varepsilon_{Hf}(t)$ values ranging from +1.4 to +4.9, and T_{DM2} model ages of 2.94–2.74 Ga (Fig. 10a). These features indicate that the zircon grains crystallized from magmas generated during partial melting of late Mesoarchean to early Neoarchean (2.9–2.7 Ga) juvenile crust, suggesting significant crustal growth along the northeastern margin of the Eastern Block at this time, consistent with recent studies of the NCC (Wu et al., 2005, 2013, 2015; Jahn et al., 2008; Jiang et al., 2010; Wan et al., 2010, 2011a; Geng et al., 2012). The largest group of zircon grains (2398–1856 Ma) and those with ages of 1789–1761 Ma have negative $\varepsilon_{Hf}(t)$ values of −6.7 to −1.4 and −6.5 to −0.5, respectively. T_{DM2} model ages for the 2398–1856 Ma zircon grains range from 3.17 to 2.62 Ga, and those for the 1789–1761 grains range from 2.84 to 2.48 Ga (Fig. 10a), which are significantly older than their U–Pb ages, indicating that these grains were derived from the reworking of Mesoarchean to early Neoarchean crust. Combining the Hf isotopic data with the regional geology of the north-eastern margin of the Eastern Block, we conclude that the major crustal growth event in this region occurred between the Mesoarchean and Neoarchean (3.2–2.5 Ga), with a peak at 2.9–2.7 Ga (Fig. 10b).

7 Conclusions

(1) Regional stratigraphic correlation indicates that

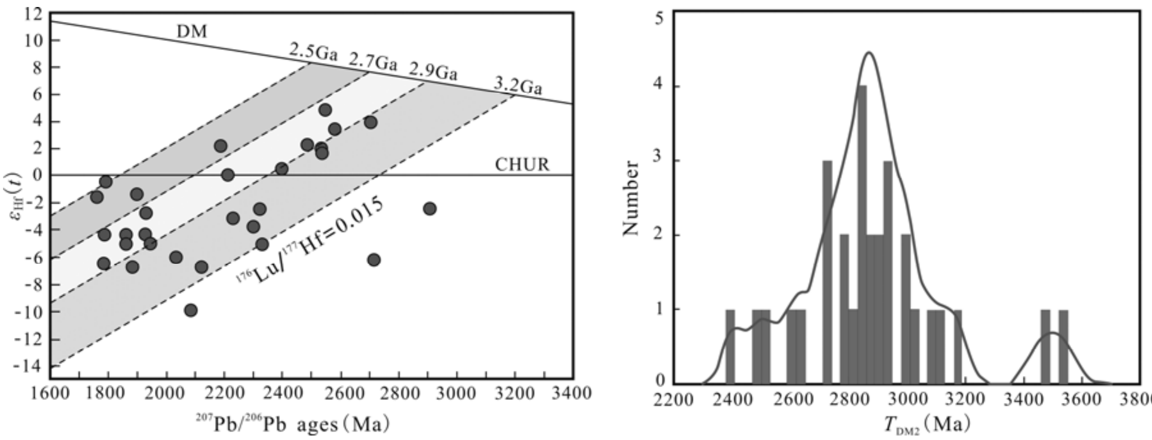

Fig. 10. Zircon $^{207}Pb/^{206}Pb$ ages versus $\varepsilon_{Hf}(t)$ values for zircon grains from sample RZ43.

much of the Lujiapuzi Formation is equivalent to the Tuanshanzi Formation, and has a depositional age of <1780 Ma.

(2) Archean basement of the Longgang Block and the Paleoproterozoic Liao-Ji Belt were the principal sources of sediment in the Lujiapuzi Formation.

(3) The base of the Changcheng System in the Yan-Liao Rift has an age of ca. 1.80 Ga.

(4) The major crustal growth event along the northeastern margin of the Eastern Block occurred between the Mesoarchean and Neoarchean (3.2–2.5 Ga), with a peak at 2.9–2.7 Ga.

Acknowledgements

We thank editor and two anonymous reviewers for their thorough reviews and constructive comments. We are grateful to the staff of the Beijing Zhongshi Geological Analysis Laboratories of China, for advice and assistance on the U–Pb zircon dating by LA–ICP–MS. We also thank the staff of the Shenyang Mineral Resources Supervision and Inspection Center of China, for their assistance on the major and trace element analyses. This study was financially supported by the Nature Science Foundation of China (41772214 and 41872203), the 12th Chinese 1000 Young Talents Program, National Nature Science Foundation of China (2016-67, 32020002), and the China Postdoctoral Science Foundation Grant (2018M633210) and the China Geological Survey (12120113057900).

Manuscript received Mar. 22, 2018
accepted May 22, 2018
edited by Fei Hongcai

References

Blichert-Toft, J., and Albarede, F., 1997. The Lu-Hf isotope geochemistry of chondrites and the evolution of the mantle-crust system. *Earth Planetary Science Letters*, 148: 243–258.

Böhm, C.O., Heaman, L.M., Creaser, R.A., and Corkery, M.T., 2000. Discovery of pre-3.5 Ga exotic crust at the northwestern Superior Province margin, Manitoba. *Geology*, 28(1): 75–78.

Cai Jianhui, Yan Guohan., Mu Baolei, Xu Baoling, Shao Hongxiang and Xu Ronghua, 2002. U-Pb and Sm-Nd isotopic ages of an alkaline syenite complex body in Liangtun-Kuangdonggou, Gai County, Liaoning Province, China and their geological significance. *Acta Petrologica Sinica*, 18(3): 349–354 (in Chinese with English abstract).

Cawood, P.A., and Nemchin, A.A., 2000. Provenance record of a rift basin: U/Pb ages of detrital zircons from the Perth Basin, Western Australia. *Sedimentary Geology*, 134(3–4): 209–234.

Condie K.C., Belousova E., Griffin W.L., and Sircombe K.N., 2009. Granitoid events in space and time: Constraints from igneous and detrital zircon age spectra. *Gondwana Research,* 15(3–4): 228–242.

Chen Bin, Li Zhuang, Wang Jialing, Zhang Lu and Yan Xuelong, 2016. Liaodong Peniusula ~2.2Ga magmatic event and its geological significance. *Journal of Jilin University* (Earth Science Edition), 46(2): 303–320 (in Chinese with English abstract).

Chen Yuejun, Peng Yujing, Liu Yuewen and Matthew, G., 2006. Progress in the study of chronostratigraphy of the “Qinghezhen Group”. *Geological Review*, 52(2): 171–177 (in Chinese with English abstract).

Diwu Chunrong, Sun Yong, Lin Ciluan, Liu Xiaoming and Wang Hongliang, 2007. Zircon U-Pb ages and Hf isotopes and their geological significance of Yiyang TTG gneisses from Henan province, China. *Acta Petrologica Sinica*, 23(2): 253–262 (in Chinese with English abstract).

Duan Chao, Li Yanhe, Wei Minghui, Yang Yun, Hou Kejun, Chen Xiaodan and Zou Bin, 2014. U-Pb dating study of detrital zircons from the Chuanlinggou Formation in Jiangjiazhai iron deposit, North China Craton and its geological significances. *Acta Petrologica Sinica*, 30(1): 35–48 (in Chinese with English abstract).

Gao Linzhi, Zhang Chuanheng, Shi Xiaoying, Zhou Hongrui and Wang Ziqiang, 2007. Zircon SHRIMP U-Pb dating of the tuff bed in the Xiamaling Formation of the Qingbaikouan System in North China. *Geological Bulletin of China*, 26(3): 249–255 (in Chinese with English abstract).

Gao Linzhi, Zhang Chuanheng, Yin Chongyu, Shi Xiaoying, Wang Ziqiang, Liu Yaoming, Liu Pengju., Tang Feng and Song Biao, 2008. SHRIMP zircon ages: basis for refining the chronostratigraphic classification of the Meso-and Neoproterozoic strata in North China Old Land. *Acta Geoscientica Sinica*, 29(3): 366–376 (in Chinese with English abstract).

Gehrels, G., 2014. Detrital Zircon U-Pb geochronology applied to tectonics. *Annual Review of Earth and Planetary Sciences*, 42(1): 127–149.

Geng Yuansheng, Du Lilin and Ren Liudong, 2012. Growth and reworking of the early Precambrian continental crust in the North China Craton: Constraints from zircon Hf isotopes. *Gondwana Research*, 21(2–3): 517–529.

Geng Yuansheng, Liu Dunyi and Song Biao, 1997. Chronological framework of the early Precambrian important events of the Northwestern Hebei granulite terrain. *Acta Geologica Sinica*, 71(4): 316–327 (in Chinese with English abstract).

Geng Yuansheng, Yang Chonghui and Wan Yusheng, 2006. Paleoproterozoic granitic magmatism in the Lüliang area, North China Craton: Constraint from isotopic geochronology. *Acta Petrologica Sinica*, 22(2): 305–314 (in Chinese with English abstract).

Geslin, J.K., Link, P.K., and Fanning, C.M., 1999. High-precision provenance determination using detrital-zircon ages and petrography of Quaternary sands on the eastern Snake River Plain, Idaho. *Geology*, 27(4): 295–298.

Griffin, W.L., Belousova, E.A., Shee, S.R., Pearson, N.J., and O’Reilly, S.Y., 2004. Archean crustal evolution in the northern Yilgarn Craton: U-Pb and Hf-isotope evidence from detrital zircons. *Precambrian Research*, 131: 231–282.

Griffin, W.L., Pearson, N.J., Belousova, E.A., Jackson SE, van Achterbergh E, O’Reilly S.Y., and Shee S.R., 2000. The Hf isotope composition of cratonic mantle: LAM-MC-ICPMS analysis of zircon megacrysts in kimberlites. *Geochimic Et Cosmochimic Acta*, 64(1): 133–147.

Guan Hong, Sun Min, Wilde S.A., Zhou Xinhua and Zhai Mingguo, 2002. SHRIMP U-Pb zircon geochronology of the Fuping Complex: implications for formation and assembly of the North China Craton. *Precambrian Research*, 113: 1–18.

He Zhengjun, Niu baogui, Zhang Xinyuan, Zhao Lei and Liu Renyan, 2011. Discovery of the paleo-weathered mantle of the rapakivi granite covered by the Proterozoic Changzhougou Formation in the Miyun area, Beijing and their detrital zircon dating. *Geological Bulletin of China*, 30(3–4): 798–802 (in Chinese with English abstract).

Hu Junliang, Zhao Taiping, Xu Yonghang and Chen Wei, 2007. Geochemistry and petrogenesis of the high-K volcanic rocks in the Dahongyu Formation, North China Craton. *Journal of Mineralogy and Petrology*, 27(4): 70–77 (in Chinese with English abstract).

Hu Zhaochu, Gao Shan, Liu Yongsheng, Hu Shenghong, Chen Haihong and Yuan Honglin, 2008. Signal enhancement in laser ablation ICP-MS by addition of nitrogen in the central channel gas. *Journal of Analytical Atom Spectrometry*, 23(8): 1093–1101.

Huang Daomao, Zhang Dehui, Wang Shiyan, Zhang Yixin, Dong Chunyan, Liu Dunyi and Wan Yusheng, 2012. 2.3 Ga magmatism and 1.94 Ga metamorphism in the Xiatang area, southern margin of the North China craton: Evidence from whole-rock geochemistry and zircon geochronology and Hf isotope. *Geological Review*, 58(3): 565–576 (in Chinese with English abstract).

Huang Xiaolong, Wilde, S.A., Yang Qijun and Zhong Junwei, 2012. Geochronology and petrogenesis of gray gneisses from the Taihua Complex at Xiong'er in the southern segment of the Trans-North China Orogen: Implications for tectonic transformation in the Early Paleoproterozoic. *Lithos*, 134–135: 236–252.

Jahn, B.M., Liu Dunyi, Wan Yusheng, Song Biao and Wu Jiashan, 2008. Archean crustal evolution of the Jiaodong Peninsula, China, as revealed by zircon SHRIMP geochronology, elemental and Nd-isotope geochemistry. *American Journal Sciences*, 308(3): 232–269.

Jiang Neng, Guo Jinghui, Zhai Mingguo and Zhang Shuangquan, 2010. ~2.7 Ga crust growth in the North China craton. *Precambrian Research*, 179(1): 37–49.

Jiang Zongsheng, Wang Guodong, Xiao Lingling, Diwu Chunrong, Lu Junsheng and Wu Chunming, 2011. Paleoproterozoic metamorphic P-T-t path and tectonic significance of the Luoning metamorphic complex at the southern terminal of the Trans-North China Orogen, Henan Province. *Acta Petrologica Sinica*, 27(12): 3701–3717 (in Chinese with English abstract).

Kinny, P.D., Compston, W., and Williams, I.S., 1991. A reconnaissance ion–probe study of hafnium isotopes in zircons. *Geochimica Et Cosmochimica Acta*, 55(3): 849–859.

Kinny, P.D., and Maas, R., 2003. Lu-Hf and Sm-Nd isotope systems in Zircon. In: Hanchar, J.M., Hoskin, P.W.O. (Eds.), *Reviews in Mineralogy and Geochemistry*, 53(1): 327–341.

LBGMR (Liaoning Bureau of Geology and Mineral Resources), 1976. *1:200 000 scale geological maps of the Kaiyuan, Liaoning and the related notes* (in Chinese).

LBGMR (Liaoning Bureau of Geology and Mineral Resources), 1988. *Regional geological records of Liaoning Province* (in Chinese).

LBGMR (Liaoning Bureau of Geology and Mineral Resources), 1993. *1:50 000 scale geological maps of Niejiagou and Diaopitun, Liaoning and the related notes* (in Chinese).

LBGMR (Liaoning Bureau of Geology and Mineral Resources), 2015. *Regional geological records of Liaoning Province* (in Chinese).

Li Huaikun, Li Huimin and Lu Songnian, 1995. Grain zircon U–Pb age for volcanic rocks from Tuanshanzi Formation of Changcheng System and their geological implication. *Geochimica*, 24(1): 43–48 (in Chinese with English abstract).

Li Huaikun, Lu Songnian, Su Wenbo, Xiang Zhenqun, Zhou Hongying and Zhang Yongqing, 2013. Recent advances in the study of the Mesoproterozoic geochronology in the North China Craton. *Journal of Asian Earth Sciences*, 72(4): 216–227.

Li Huaikun, Lu Songnian, Li Huimin, Sun Lixin, Xiang Zhenqun, Geng Jianzhen and Zhou Hongying, 2009. Zircon and beddeleyite U-Pb precision dating of basic rock sills intruding Xiamaling Formation, North China. *Geological Bulletin of China*, 28(1): 1396–1404 (in Chinese with English abstract).

Li Huaikun, Su Wenbo, Zhou Hongying, Geng Jianzhen, Xiang Zhenqun, Cui Yurong, Liu Wenchan and Lu Songnian, 2011. The base age of Changchengian System at the northern North China Craton should be younger than 1670 Ma: constraints from zircon U-Pb LA-MC-ICP MS dating of a granite porphyry dike in Miyun County, Beijing. *Earth Science Frontiers*, 18(3): 108–120 (in Chinese with English abstract).

Li Huaikun, Su Wenbo, Zhou Hongying, Xiang Zhenqun, Tian Hui, Yang Ligong, Warren, D.H., and Frank, R.E., 2014. The first precise age constraint on the Jixian System of the Meso- to Neoproterozoic Standard Section of China, SHRIMP zircon U-Pb dating of bentonites from the Wumishan and Tieling formations in the Jixian Section, North China. *Acta Petrologica Sinica*, 30(10): 2999–3012 (in Chinese with English abstract).

Li Huaikun, Zhu Shixing, Xiang Zhenqun, Su Wenbo, Lu Songnian, Zhou Hongying, Geng Jianzhen, Li Sheng and Yang Fengjie, 2010. Zircon U-Pb dating on tuff bed from Gaoyuzhuang Formation in Yanqing, Beijing: Further constraints on the new subdivision of the Mesoproterozoic stratigraphy in the northern North China Craton. *Acta Petrologica Sinica*, 26(7): 2131–2140 (in Chinese with English abstract).

Li Sanzhong and Zhao Guochun, 2007. SHRIMP U-Pb zircon geochronology of the Liaoji granitoids: Constraints on the evolution of the Paleoproterozoic Jiao-Liao-Ji belt in the Eastern Block of the North China Craton. *Precambrian Research*, 158: 1–16.

Li Tong, 1994. Element abundances of China's continental crust and sedimentary layer and upper continental crust. *Geochimica*, 23: 140–145 (in Chinese with English abstract).

Li Zhuang, Chen Bin, Liu Jingwei, Zhang Lu and Yang Chuan, 2015, Zircon U-Pb ages and their implications for the South Liaohe Group in the Liaodong Peninsula, Northeast China. *Acta Petrologica Sinica*, 31(6): 1589–1605 (in Chinese with English abstract).

Li Zhuang, Chen Bin and Wang Jialin, 2016. Geochronological framework and geodynamic implications of mafic magmatism in the Liaodong peninsula and adjacent regions, North China Craton. *Acta Geologica Sinica* (English Edition), 90(1): 138–153.

Liu Chaohui, Zhao Guochun, Liu Fulai and Shi Jianrong, 2017a. Detrital zircon U-Pb and Hf isotopic and whole-rock geochemical study of the Bayan Obo Group, northern margin of the North China Craton: Implications for Rodinia reconstruction. *Precambrian Research*, 303: 372–391.

Liu Dunyi, Nutman, A.P., Compston, W., Wu Jiashan and Shen Qihan, 1992. Remnants of ≥3800 Ma crust in the Chinese part of the Sino-Korean craton. *Geology*, 20(4): 339–342.

Liu Dunyi, Nutman, A.P., Williams, I.S., Compston, W., Wu Jiashan and Shen Qihan, 1994. The remnants of ≥3800 Ma crust in Sino-Korean Craton-The evidence from ion microprobe U-Pb dating of zircons. *Acta Geoscientia Sinica*, 1–2: 3–13 (in Chinese with English abstract).

Liu Dunyi, Wilde, S.A., Wan Yusheng, Wu Jiashan, Zhou Hongying, Dong Chunyang and Yin Xiaoyan, 2008. New U-Pb and Hf isotopic data confirm Anshan as the oldest preserved segment of the North China Craton. *American Journal of Science*, 308: 200–231.

Liu Fulai, Liu Chaohui, Itano, K., Iizuka, T., Cai Jia and Wang Fang, 2017b. Geochemistry, U-Pb dating, and Lu-Hf isotopes of zircon and monazite of porphyritic granites within the Jiao-Liao-Ji orogenic belt: Implications for petrogenesis and tectonic setting. *Precambrian Research*, 300: 78–106.

Liu Jin, 2017. *The Mesozoic tectonic evolution of Kuaiyuan Area in the eastern segment of northern margin of the North China Block*. Changchun: Jilin University (Ph. D thesis): 1–136 (in Chinese with English abstract).

Liu Jin, Li Dongtao, Kuai Bin, Li Yuchao, Peng Youbo, Zhao Chen, Yang Zhongjie and Liu Wenbin, 2013. Mesoproterozoic orogenic belt in the east part of the Northern margin of North China Plate: Geologic characteristics of tectonic evolution. *Geology and Resources*, 22: 435–443 (in Chinese with English abstract).

Liu Jin, Liu Zhenghong, Li Shichao, Zhao Chen, Wang Chujie, Peng Youbo, Yang Zhongjie and Dou Shiyong, 2016. Geochronology and geochemistry of Triassic intrusive rocks in Kaiyuan area of the eastern section of the northern margin of North China. *Acta Petrologica Sinica*, 32: 2739–2756 (in Chinese with English abstract).

Liu Jin, Liu Zhenghong, Zhao Chen, Peng Youbo, Wang Chujie, Yang Zhongjie and Dou Shiyong, 2017. Discovery of the late Archean Supracrustal rock to the north of Qinghe fault in Liaoning province and its geological significance. *Journal of Jilin University (*Earth Science Edition*)*, 47: 497–510 (in Chinese with English abstract).

Liu Jin, Liu Zhenghong, Zhao Chen, Wang Chujie and Peng Youbo, 2017c. Petrogenesis and zircon U–Pb LA–ICP–MS dating of newly discovered Mesoarchean tonalitic gneiss in the Luanjiajie area of northern Liaoning Province, China. *International Geology Review*, 59: 1575–1589.

Liu Jin, Liu Zhenghong, Zhao Chen, Wang Chujie, Guan Qingbin, Dou Shiyong and Song Shue, 2017d. Geochemistry and U-Pb detrital zircon ages of late Permian to Early Triassic metamorphic rocks from northern Liaoning, North China: Evidence for the timing of final closure of the Paleo-Asian Ocean. *Journal of Asian Earth Science*, 145: 460–474.

Liu Jin, Zhang Jian, Liu Zhenghong, Yin Changqing, Zhao Chen, Li Zhuang, Yang Zhongjie and Dou Shiyong, 2018. Geochemical and geochronological study on the Paleoproterozoic rock assemblage of the Xiuyan region: New constraints on an integrated rift-and-collision tectonic process involving the evolution of the Jiao-Liao-Ji belt, North China Craton. *Precambrian Research*, 310: 179–197.

Liu Shuwen, Santosh, M., Wang Wei, Bai Xiang and Yang Pengtao, 2011. Zircon U-Pb chronology of the Jianping Complex: Implications for the Precambrian crustal evolution history of the northern margin of North China Craton. *Gondwana Research*, 20(1): 48–63.

Liu Yongsheng, Gao Shan, Hu Zhaochu, Gao Changgui, Zong keqing and Wang Dongbing, 2010. Continental and oceanic crust recycling-induced melt-peridotite interactions in the Trans-North China Orogen. U-Pb dating, Hf isotopes and trace elements in zircons from mantle xenoliths. *Journal of Petrology*, 51: 537–571.

Liu Yongsheng, Hu Zhaochu, Gao Shan, Gunther, D., Xu Juan, Gao Changgui and Chen Haihong, 2008. In situ analysis of major and trace elements of anhydrous minerals by LA-ICP-MS without applying an internal standard. *Chemical Geology*, 257(1–2): 34–43.

Liu Zhenghong, Cheng Liren, Xu Zhongyuan and Zheng Changqing, 1999a. The discovery and significance of mircropaleontological fossils in marbles in primary Jianping Group at northern Fuxin, western Liaoning Province. *World Geology*, 18(2): 30–34 (in Chinese with English abstract).

Liu Zhenghong, Xu Zhongyuan and Yang Zhensheng, 1999b. Establishment of the middle Proterozoic Weijiagou rock group and the geological significance in the north margin of North China Platform. *Journal of Changchun University of Science and Technology*, 29(1): 9–14 (in Chinese with English abstract).

Ludwig, K.R., 2003. User's manual for Isoplot 3.0: A geochronological toolkit for Microsoft Excel. *Berkeley Geochronology Center Special Publication, Berkeley, CA*, 4: 1–20.

Lu Songnian, Yang Chuanliang, Li Huaikun and Li Humin, 2002. A group of rifting events in the terminal Paleoproterozoic in the North China Craton. *Gondwana Research*, 5(1): 123–131.

Lu Songnian, Li Huaikun, Li Huimin, Song Biao, Wang Shiyan, Zhou Hongying and Chen Zhihong, 2003. U-Pb isotopic ages and their significance of alkaline granite in the southern margin of the North China Craton. *Geological Bulletin of China*, 22(10): 762–768 (in Chinese with English abstract).

Lu Songnian, Zhao Guochun, Wang Huichu and Hao Guojie, 2008. Precambrian metamorphic basement and sedimentary cover of the North China Craton: A review. *Precambrian Research*, 160: 77–93.

Lu Xiaoping, Wu Fuyuan, Lin Jingqian, Sun Deyou, Zhang Yanbin and Guo Chunli, 2004a. Geochronological successions of the early Precambrian granitic magmatism in southern Liaodong Peninsula and its constraints on tectonic evolution of the North China Craton. *Chinese Journal of Geology*, 38 (1): 123–138 (in Chinese with English abstract).

Lu Xiaoping, Wu Fuyuan, Zhang Yanbin, Zhao Chengbi and Guo Chunli, 2004b. Emplacement age and tectonic setting of the Paleoproterozoic Liaoji granites in Tonghua area, south Jilin province. *Acta Petrologica Sinica*, 20(3): 381–392 (in Chinese with English abstract).

Lu Xiaoping, Wu Fuyuan, Guo Jinghui and Yin Changjian, 2005. Paleoproterozoic granitic magmatism and crustal evolution in the Tonghua region, northeast China. *Acta Petrologica Sinica*, 21(3): 721–736 (in Chinese with English abstract).

Lu Xiaoping, Wu Fuyuan, Guo Jinghui, Wilde, S.A., Yang Jinhui, Liu Xiaoming and Zhang Xiaoou, 2006. Zircon U-Pb geochronological constraints on the Paleoproterozoic crustal evolution of the Eastern Block in the North China Craton. *Precambrian Research*, 146(3-4): 138–164.

Mao Debao, Zhong Changting, Chen Zhihong, Lin Yuanxian, Li Huimin and Hu Xiaodie, 1999. The isotopic ages and geological implications of high-pressure mafic granulites in the northern Chengde area, Hebei Province, China. *Acta Petrologica Sinica*, 15(4): 524–534 (in Chinese with English abstract).

Meng En, Liu Fulai, Liu Pinghua, Liu Chaohui, Yang Hong, Wang Fang, Shi Jianrong and Cai Jia, 2014. Petrogenesis and tectonic significance of Paleoproterozoic meta-mafic rocks from central Liaodong Peninsula, northeast China: evidence from zircon U-Pb dating and in situ Lu-Hf isotopes, and whole-rock geochemistry. *Precambrian Research*, 247(1): 92–109.

Peng Peng, Zhai Mingguo, Li Qiuli, Wu Fuyuan, Hou Quanlin, Li Zhong, Li Tiesheng and Zhang Yanbin, 2011. Neoproterozoic (~900 Ma) Sariwon sills in North Korea: geochronology, geochemistry and implications for the evolution of the south-eastern margin of the North China Craton. *Gondwana Research*, 20(1): 243–254.

Peng Peng, Zhai Mingguo, Ernst, R.E., Guo Jinghui, Liu Fu and Hu Bo, 2008. A 1.78 Ga large igneous province in the North China craton: The Xiong'er Volcanic Province and the North China dyke swarm. *Lithos*, 101(3–4): 260–280.

Peng Peng, Liu Fu, Zhai Mingguo and Guo Jinghui, 2012. Age of the Miyun dyke swarm: Constraints on the maximum depositional age of the Changcheng System. *Chinese Science Bulletin*, 57(1): 105–110.

Qi Liang, Hu Jing and Gregoire, D.C., 2000. Determination of trace elements in granites by inductively coupled plasma-mass spectrometry. *Talanta*, 51(3): 507–513.

Qiao Xiufu and Wang Yanbin, 2014. Discussions on the lower boundary age of the Mesoproterozoic and basin tectonic evolution of the Mesoproterozoic in the North China Craton. *Acta Geologica Sinica*, 88(9): 1623–1637 (in Chinese with English abstract).

Ren Rong, Han Baofu, Zhang Zhicheng, Li Jianfeng, Yang Yueheng and Zhang Yanbin, 2011. Zircon U-Pb and Hf isotopic studies of basement gneiss and overlying Meso-Neoproterozoic sedimentary rocks from the Changping area, Beijing, and their geological implications. *Acta Petrologica Sinica*, 27(6): 1721–1745 (in Chinese with English abstract).

Santosh, M., Sajeev, K., and Li, J.H., 2006. Extreme crustal metamorphism during Columbia supercontinent assembly: evidence from North China Craton. *Gondwana Research*, 10 (3–4): 256–266.

Santosh, M., Tsunogae, T., Li, J.H., and Liu, S.J., 2007. Discovery of sapphirine-bearing Mg–Al granulites in the North China Craton: implications for Paleoproterozoic ultrahigh temperature metamorphism. *Gondwana Research*, 11(3): 263–285.

Santosh, M., 2010. Assembling North China Craton within the Columbia supercontinent: the role of double-sided subduction. *Precambrian Research*, 178(1–4): 149–167.

Scherer, E.E., Munker, C., and Mezger, K., 2001. Calibration of the Lutetium-hafnium clock. *Science*, 293: 683–687.

Shi Yuruo and Zhao Xitao, 2017. Early Neoarchean magmatic and Paleoproterozoic metamorphic events in the northern North China Craton: SHRIMP zircon dating and Hf isotopes of Archean rocks from the Miyun Area, Beijing. *Acta Geologica Sinica* (English Edition), 91(3): 988–1002.

Simonen, A., 1953. Stratigraphy and sedimentation of the Svecofennidie, early Archean supracrustal rocks in southwestern Finland. *Bulletin of the Geological Society of Finland*, 160: 1–64.

Song Jian, Liu Zhihong, Wang Chao, Gao Xiang and Sun Linan, 2018. Constraints of the Jiapigou gneiss complex over evolution of the Archean Terrain in southern Jilin province: evidence from petrography, geochemistry, and U-Pb chronology analysis. *Acta Geologica Sinica*, 92(5): 908–927 (in Chinese with English abstract).

Su Wenbo, Zhang Shihong, Huff, W.D., Li Huaikun, Ettensohn, F.R., Chen Xiaoyu, Yang Hongmei, Han Yigui, Song Biao and Santosh, M., 2008. SHRIMP U-Pb ages of K-bentonite beds in the Xiamaling Formation: Implications for revised subdivision of the Meso-to Neoproterozoic history of the North China Craton. *Gondwana Research*, 14(3): 543–553.

Su Wenbo, Li Huaikun, Huff, W.D., Ettensohn, F.R., Zhang Shihong, Zhou Hongying and Wan Yusheng, 2010. SHRIMP U-Pb dating for a K-bentonite bed in the Tieling Formation, North China. *Chinese Science Bulletin*, 55(29): 3312–3323 (in Chinese with English abstract).

Sun, M., Armstrong, R.L., and Lambert, R.S., 1993. Petrochemistry and Sr, Pb and Nd isotopic geochemistry of Paleoproterozoic Kuandian Complex, the Eastern Liaoning Province, China. *Precambrian Research*, 62: 171–190.

Sun, S.S., and McDonough, W.F., 1989. Chemical and isotopic systematics of oceanic basalts: Implications for mantle composition and processes. *Geological Society London Special Publications*, 42: 313–345.

Tang Jun, Zheng Yongfei, Wu Yuanbao, Gong Bing and Liu Xiaoming, 2007. Geochronology and geochemistry of metamorphic rocks in the Jiaobei terrane: Constraints on its tectonic affinity in the Sulu orogeny. *Precambrian Research*, 152(1–2): 48–82.

Tian Hui, Zhang Jian, Li Huaikun, Su Wenbo, Zhou Hongying, Yang Ligong, Xiang Zhenqun, Geng Jianzhen, Liu Huan, Zhu Shixing and Xu Zhenqing, 2015. Zircon LA-MC-ICPMS U-Pb dating of tuff from Mesoproterozoic Gaoyuzhuang Formation in Jixian County of North China and its geological significance. *Acta Geoscientica Sinica*, 63(5): 647–658 (in Chinese with English abstract).

Wan Yusheng, Liu Dunyi, Wang Shijin, Dong Chunyan, Yang Enxiu, Wang Wei, Zhou Hongying, Du Lilin, Yin Xiaoyan, Xie Hangqiang and Ma Mingzhu, 2010. Juvenile magmatism and crustal recycling at the end of Neoarchean in western Shandong Province, North China Craton: Evidence from SHRIMP zircon dating. *American Journal Sciences*, 310: 1503–1552.

Wan Yusheng, Liu Dunyi, Wang Shijin, Yang Enxiu, Wang Wei, Dong Chunyan, Zhou Hongying, Du Linli, Yang Yueheng and Diwu Chunrong, 2011a. ~2.7 Ga juvenile crust formation in the North China Craton (Taishan-Xintai area, western Shandong Province): Further evidence of an understated event from zircon U–Pb dating and Hf isotope composition. *Precambrian Research*, 186(1–4): 169–180.

Wan Yusheng, Liu Dunyi, Wang Wei, Song Tianrui, Kroner, A., Dong Chunyan, Zhou Hongying and Yin Xiaoyan, 2011b. Provenance of Meso to Neoproterozoic cover sediments at the Ming Tombs, Beijing, North China Craton: An integrated study of U-Pb dating and Hf isotopic measurement of detrital zircons and whole- rock geochemistry. *Gondwana Research*, 20(1): 219–242.

Wan Yusheng, Song Biao, Liu Dunyi, Wilde, S.A., Wu Jiashan, Shi Yurong, Yin Xiaoyan and Zhou Hongying, 2006. SHRIMP U-Pb zircon geochronology of Palaeoproterozoic metasedimentary rocks in the North China Craton: Evidence for a major Late Palaeoproterozoic tectonothermal event. *Precambrian Research*, 149(3–4): 249–271.

Wan Yusheng, Song Biao, Yang Chun and Liu Dunyi, 2005. Zircon Shrimp U-Pb geochronology of Archaean rocks from the Fushun-Qingyuan area, Liaoning province and its geological significance. *Acta Petrologica Sinica*, 79: 78–87 (in Chinese with English abstract).

Wan Yusheng, Zhang Qiaoda and Song Tianrui, 2003. SHRIMP ages of detrital zircons from the Changcheng System in the Ming Tombs area, Beijing: constraints on the protolith nature and maximum depositional age of the Mesoproterozoic cover of the North China Craton. *Chinese Science Bulletin*, 48(22): 2500–2506.

Wang Dongfang, Chen Congyun, Yang Shen, Yang Xuezeng and Zhang Jiongfei, 1988. The foundation of Early Paleozoic Qinghezhen Group in Northern Liaoning and its important geological significance. Bulletin of Shenyang Institute of Geology and Mineral Resources. *Chinese Academy of Geological Sciences*, 17: 1–21 (in Chinese).

Wang Renmin, He Gaoping, Chen Zhenzhen, Zheng Songyan and Geng Yuansheng, 1987. *Graphical method for Protolith reconstruction of metamorphic rocks*. Beijing. Geological Publishing House: 1–51.

Wang Renmin, Ni Zhiyao, Yuan Jianping and Tong Ying, 2002. More on the evidence of the paleostylolitic zone in northern Hebei Province. *Acta Petrologica et Mineralogica*, 21(4): 327 –335 (in Chinese with English abstract).

Wang Wei, Liu Shuwen, Cawood, P.A., Bai Xiang, Guo Rongrong, Guo Boran and Wang Kang, 2016a. Late Neoarchean subduction-related crustal growth in the Northern Liaoning region of the North China Craton: Evidence from ~2.55 to 2.50 Ga granitoid gneisses. *Precambrian Research*, 281: 200–223.

Wang Wei, Liu Shuwen, Santosh, M., Deng Zhengbin, Guo Boran, Zhao Yue, Zhang Shuanghong, Yang Pengtao, Bai Xiang and Guo Rongrong, 2015. Late Paleoproterozoic geodynamics of the North China Craton: Geochemical and zircon U-Pb-Hf records from a volcanic suite in the Yanliao rift. *Gondwana Research*, 27(1): 300–325.

Wang Wei, Liu Shuwen, Wilde, S.A., Li Qiugen, Zhang Jian, Bai Xiang, Yang Pengtao and Guo Rongrong, 2012. Petrogenesis and geochronology of Precambrian granitoid gneisses in Western Liaoning Province: Constraints on Neoarchean to early Paleoproterozoic crustal evolution of the North China Craton. *Precambrian Research*, 222–223: 290–311.

Wang Chaoyang, Meng En, Li Yanguang, Cai Jia, Yang Hong and Li Zhuang, 2017a. A new discovery of ~2.7 Ga granitic magmatism in southeastern Jilin Province, China. *Acta Geologica Sinica* (English Edition), 91(5): 1919–1923.

Wang Xinping, Peng Peng, Wang Chong and Yang Shuyan, 2016b. Petrogenesis of the 2115 Ma Haicheng mafic sills from the Eastern North China Craton: Implications for an intra-continental rifting. *Gondwana Research*, 39: 347–364.

Wang Xinping, Peng Peng, Wang Chong, Yang Shuyan, Söderlund, U., and Su Xiangdong, 2017b. Nature of three episodes of Paleoproterozoic magmatism (2180 Ma, 2115 Ma and 1890 Ma) in the Liaoji belt, North China with implications for tectonic evolution. *Precambrian Research*, 298: 252–267.

Wilde, S.A., and Zhao Guochun, 2005. Late Archean to Paleoproterozoic evolution of the North China Craton. *Journal of Asian Earth Sciences*, 24: 519–522.

Wilde, S.A., Zhao Guochun and Sun Min, 2002. Development of the North China Craton during the Late Archean and its final amalgamation at 1.8 Ga; some speculations on its position within a global Paleoproterozoic Supercontinent. *Gondwana Research*, 5(1): 85–94.

Wilde, S.A., Cawood, P.A., Wang, K.Y., and Nemchin, A.A., 2005. Granitoid evolution in the late Archean Wutai Complex, North China Craton. In: Wilde, S.A., Zhao, G.C. (Eds.), Late Archean to Paleoproterozoic Evolution of the North China Craton. *Journal of Asian Earth Sciences*, 24: 597–613.

Wu Fuyuan, Yang Yueheng, Xie Liewen, Yang Jinhui and Xu Ping, 2006. Hf isotopic compositions of the standard zircons and baddeleyites used in U-Pb geochronology. *Chemical Geology*, 234(1–2): 105–126.

Wu Fuyuan, Li Xianhua, Zheng Yongfei and Gao Shan, 2007. Lu–Hf isotopic systematics and their applications in petrology. *Acta Petrologica Sinica*, 23(2): 185–220 (in Chinese with English abstract).

Wu Fuyuan, Zhang Yanbin, Yang Jinhui, Xie Liewen and Yang Yueheng, 2008. Zircon U-Pb and Hf isotopic constraints on the Early Archean crustal evolution in Anshan of the North China Craton. *Precambrian Research*, 167(3–4), 339–362.

Wu Fuyuan, Zhao Guochun, Wilde, S.A., and Sun Deyou, 2005. Nd isotopic constraints on crustal formation in the North China Craton. *Journal of Asian Earth Sciences*, 24(5): 523–545.

Wu Meiling, Lin Shoufa, Wan Yusheng and Gao Jianfeng, 2015. Crustal evolution of the Eastern Block in the North China Craton: Constraints from zircon U–Pb geochronology and Lu–Hf isotopes of the Northern Liaoning Complex. *Precambrian Research*, 275: 35–47.

Wu Meiling, Zhao Guochun, Sun Min, Li Sanzhong, He Yanhong and Bao Zhian, 2013. Zircon U-Pb geochronology and Hf isotopes of major lithologies from the Yishui Terrane: Implications for the crustal evolution of the Eastern Block, North China Craton. *Lithos*, 170-171: 164–178.

Wysoczanski, R.J., Gibson, G.M., and Ireland, T.R., 1997. Detrital zircon age patterns and provenance in late Paleozoic-early Mesozoic New Zealand terranes and development of the Paleo-Pacific Gondwana margin. *Geology*, 25: 939–942.

Yang Jinhui, Wu Fuyuan, Xie Liewen and Liu Xiaoming, 2007. Petrogenesis and tectonic implications of Kuangdonggou syenites in the Liaodong Peninsula, east North China Craton: Constraints from in-situ zircon U-Pb ages and Hf isotopes. *Acta Petrologica Sinica*, 23(2): 263–276 (in Chinese with English abstract).

Yu Jiejiang, Yang Debin, Feng Hong and Lan Xiang, 2007. Chronology of amphibolite protolith in Haicheng of southern Liaoning: evidence from LA-ICP-MS zircon U-Pb dating.

Global Geology, 26(4): 391–396 (in Chinese with English abstract).

Yuan Lingling, Zhang Xiaohui, Xue Fuhong, Han Chunming, Chen Haihong and Zhai Mingguo, 2015. Two episodes of Paleoproterozoic mafic intrusions from Liaoning province, North China Craton: petrogenesis ands tectonic implications. *Precambrian Research*, 264: 119–139.

Zhai Mingguo, Bian Aiguo and Zhao Taiping, 2000. The amalgamation of the supercontinent of North China craton at the end of the Neoarchaean, and its break-up during the late Palaeoproterozoic and Mesoproterozoic. *Science in China (*Series D: Earth Sciences*)*, 43 (Suppl.): 219–232.

Zhai Mingguo, 2004. 2.1–1.7 Ga geological event group and its geotectonic significance. *Acta Petrologica Sinica*, 20(6): 1343–1354 (in Chinese with English abstract).

Zhai Mingguo and Santosh, M., 2011. The Early Precambrian odyssey of the North China Craton: a synoptic overview. *Gondwana Research*, 20(1): 6–25.

Zhai Mingguo, Guo Jinghui and Liu Wenjun, 2005. Neoarchean to paleoproterozoic continental evolution and tectonic history of the North China Craton. *Journal of Asian Earth Sciences*, 24(5): 547–561.

Zhai Mingguo, Hu Bo, Zhao Taiping, Peng Peng and Meng Qingren, 2015. Late Paleoproterozoic–Neoproterozoic multi-rifting events in the North China Craton and their geological significance: a study advance and review. *Tectonophysics*, 662 (1): 153–166.

Zhang Jian, Tian Hui, Li Huaikun, Su Wenbo, Zhou Hongying, Xiang Zhenqun, Geng Jianzhen and Yang Ligong, 2015. Age, geochemistry and zircon Hf isotope of the alkaline basaltic rocks in the middle section of the Yan-Liao aulacogen along the northern margin of the North China Craton: New evidence of the breakup of the Columbia Supercontinent. *Acta Petrologica Sinica*, 31(10): 3129–3146 (in Chinese with English abstract).

Zhang Peng, Zhao Yan, Yang Hongzhi and Kou Linlin, 2016. Discrimination and its significance of the Sizhuangguizi granite in Kuangdonggou area, eastern Liaoning Province. *Journal of Northeastern University* (Natural Science), 37(9): 1349–1352 (in Chinese with English abstract).

Zhang Shuanhong, Zhao Yue, Ye Hao, Hu Jianmin and Wu Fei, 2013. New constraints on ages of the Chuanlinggou and Tuanshanzi formations of the Changcheng system in the Yan-Liao area in the northern North China Craton. *Acta Petrologica Sinica*, 29(7): 2481–2490 (in Chinese with English abstract).

Zhao Fengqing, Li Huaimin, Zuo Yicheng and Xue Keqin, 2006. Zircon U-Pb ages of Paleoproterozoic granitoids in the Zhongtiao Mountains, southern Shanxi, China. *Geological Bulletin of China*, 25(4): 442–447 (in Chinese with English abstract).

Zhao Guochun, Wilde, S.A., Cawood, P.A., and Sun Min, 2001. Archean blocks and their boundaries in the North China Craton: Lithological, geochemical, structural and P–T path constraints and tectonic evolution. *Precambrian Research*, 107(1): 45–73.

Zhao Guochun, Wilde, S.A., Sun Min, Li Sanzhoong, Li Xuping and Zhang Jian, 2008. SHRIMP U-Pb zircon ages of granitoid rocks in the Lüliang Complex: Implications for the accretion and evolution of the Trans-North China Orogen. *Precambrian Research*, 160(3): 213–226.

Zhao Guochun, Sun Min, Wilde, S.A., and Li Sanzhong, 2005. Late Archean to Proterozoic evolution of the North China Craton: Key issues revisited. *Precambrian Research*, 136(2): 177–202.

Zhao Guochun, Li Sanzhong, Sun Min and Wilde, S.A., 2010. Assembly, accretion, and break-up of the Palaeo-Mesoproterozoic Columbia supercontinent: Record in the North China Craton revisited. *International Geology Review*, 53(11–12): 1331–1356.

Zhao Guochun, Cawood, P.A., Li Sanzhong, Wilde, S.A., Sun Min, Zhang Jian, He Yanhong and Yin Changqing, 2012. Amalgamation of the North China Craton: Key issues and discussions. *Precambrian Research*, 222–223(12): 55–76.

Zhao Jiao, Zhang Chengli, Guo Xiaojun, Liu Xinyu and Wang Quan, 2015. Determination of the 2.4Ga A-type granite in Lüliang area of the North China Craton and its geological significance. *Acta Petrologica Sinica*, 31(6): 1606–1620 (in Chinese with English abstract).

Zhao Taiping, Zhou Meifu, Zhai Mingguo and Xia Bin, 2002. Paleoproterozoic rift-related volcanism of the Xiong'er group, North China craton: implications for the breakup of Columbia. *International Geology Review*, 44(4): 336–351.

Zhao Taiping, Zhai Mingguo, Xia Bin, Li Huimin, Zhang Yixing and Wan Yusheng, 2004. Zircon U-Pb SHRIMP dating for the volcanic rocks of the Xiong'er Group: constraints on the initial formation age of the cover of the North China Craton. *Chinese Science Bulletin*, 49(23): 2495–2502.

About the first author

LIU Jin, male; born in 1986 in Chongqing City; postdoctoral fellow of School of Earth Sciences and Engineering, Sun Yat-sen University. He is now work on regional geological survey and interested in the study on evolution of the North China Craton. Email: 329641912@qq.com; phone: 15942039295.